MSc Program
Renewable Energy Systems

Non-disruptive detection of Potential Induced Degradation at a utility scaled PV-power plant in Europe

A Master's Thesis submitted for the degree of
“Master of Science”

supervised by
Gerhard Mütter, Msc

DeMarsh Scott, Bsc

01249276

Vienna, 26.11.2018

Affidavit

I, **DEMARSH SCOTT, BSC**, hereby declare

1. that I am the sole author of the present Master's Thesis, "NON-DISRUPTIVE DETECTION OF POTENTIAL INDUCED DEGRADATION AT A UTILITY SCALED PV-POWER PLANT IN EUROPE", 87 pages, bound, and that I have not used any source or tool other than those referenced or any other illicit aid or tool, and
2. that I have not prior to this date submitted this Master's Thesis as an examination paper in any form in Austria or abroad.

Vienna, 26.11.2018

_____

Signature

Abstract

The purpose of this study is to present a non-disruptive form of detection into the existence of Potential Induced Degradation from monitoring data on a utility scaled PV power plant in Europe. Monitoring data is using to detect changes in performance, preliminary to any application of the more commonly utilized methods of lab testing. Promoting a reduction in downtime of affected strings and plant performance is desired.

With the growth of the PV plants worldwide taking an increasingly bigger role in energy production from the yet limitless supply produced by the Sun, our attempt to utilize and redistribute this energy for storage in batteries and for everyday consumption, poses a direct challenge in itself. This takes the form of aging modules occurring naturally with time or prematurely from internal or external sources. Si (silicon) wafer technology dominates 90% of the market and has a guarantee and lifespan of 25yrs with expected degradation rates of .8% per year, the degradation phenomena is also experienced with these types of capture media and its systems of photovoltaics. Becoming more efficient and self reliant gives rise to unexpected occurrences, Potential Induced Degradation on large scale installations is a growing concern for owners and operators. Modules tend to degrade in various ways: from high humidity, back sheet degradation, sodium ions flowing incorrectly and escaping through the glass encapsulant resulting in a form of PID. The following site study has revealed that there is no significant impact from the analysed and detected strings at the PV plant.

The aim of this paper will be a focus on one of the available and least expensive methods of PID detection with the least disruption to daily operations on a large scaled PV site; this method utilizes monitoring data to detect levels of losses and to attempt to produce early warning signs as seen in the data.

Contents

1. Introduction

The problem of Potential Induced degradation is a growing phenomenon and will need attention in its onset to prevent proliferation across a PV plant. The growth will bring a decrease in power from the site that may be recognised not from physical inspection of the modules but from output data. Comparisons of expected output against actual output should reveal this phenomenon. Testing has to be undertaken to identify the source of these losses. First steps include identifying the string of modules most affected. Identification of the affected strings is not as simple as a walk around inspection, attempting to find PID effects visually on a site containing 4000 modules arranged in 200 strings will prove an overwhelmingly daunting task to the most trained eye and would yield very little results. Furthered by the fact that PID's effects are not easily visible to the naked eye, the challenge becomes palpably greater if such a task has to be undertaken in a 100MW PV Park containing 400, 000 modules arranged in 20,000 strings .

In spite of susceptibility testing at system level that may include IR (thermographic) inspection and I-V curve measurements normally identifying affected cells at the source (manufacturers). Quality control testing would have been performed in laboratories which attempt to replicate outdoor conditions under the ambit of testing standards such as IEC 62804.It is clear modules may still become infected with PID.

PID can be reversible in the case of polarization or irreversible where there is electro chemical corrosion, (Pingel et al.2010, 1) having conducted several Laboratory tests in a climatic chamber under specific conditions which attempted to replicate the effects of temperature and humidity at cell level confirm this fact.

1.1 Motivation and History

A PV plant in Europe is being affected by Potential Induced Degradation; it is unknown to what extent they have been affected by PID. The desired task is to detect PID from the monitoring data, demonstrating its existence through the losses in output. Long term production losses will be evaluated. In addition days of high production with high irradiation values, and similar environmental conditions that may exacerbate the condition will be examined.

1.2 Core Objectives

The core objectives of this study are to

confirm recurring production losses from acquired monitoring data. Secondly to determine from an extracted dataset, what the losses are as a result of PID, and if they hold a particular discernible pattern, that is visible from the monitoring data. A third objective is to verify efficiency of PID boxes against the effects of PID. Lastly to ascertain if environmental parameters such as high temperatures, high wind speed from provided data sets have impacts on module performance.

1.3 Problem statement

A large utility sized PV plant has recognised a problem exists at the production end of their plant, after testing the diagnosis realised is Potential Induced Degradation. Measures have been taken to rectify the problem. How effective these measures have been in fully reversing or remediating the effects of PID is unclear. The challenge of identifying from acquired data sets and quantification of the losses accrued from PID in a non-invasive manner is ideal for this site. Strings impacted by PID as well as those uninfected are already known. Tracking PID's development with overlapping effects such as module temperature is key to inhibiting further infection on site. It is thought that Potential induced degradation is ranked above standard degradation. Whereas standard degradation is considered linear in growth, PID is considered exponential and as such requires greater attention from the owners and operators of a large PV Plant. It is now important for the owners and operators to be able improve or correct the current remediation process, by recovering the affected modules and halting the infection across the strings at the plant.

1.4 Methodology

The objectives of this study are to track the development of daily, weekly, monthly losses over time by showing the distribution of the intensity of losses. By plotting hourly, daily monthly production values at different irradiation, temperature, and wind speeds values the relative losses will be demonstrated, by simultaneously comparing known affected PID strings to that of neighbouring unaffected good strings. The difference will be demonstrated by the relative difference in performance of the affected (PID) and unaffected strings. This representation will be expressed as a percentage. In the process the illustration of the losses (possibly residual), even after the repair process was initiated, will be seen. By comparing the results to those claimed by the manufacturers after use of their product the effectiveness of the product should be also illustrated.

The final two objectives are to attempt to develop an early detection system through patterning of filtered data, by filtering the acquired datasets that have registered no winds speeds and temperature (+/-5°C in temperature), the influences of weather that could exacerbate PID should in theory produce a discernible pattern. Illustrating the added effects attributable to weather in the plant. Lastly to extrapolate the losses or benefits experienced at this site onto a plant of 10MW capacity for future reference.

1.5 PV Plant Description

The PV power plant is located in Europe, its construction started on the 05.07.2013 with part 2 of the site being constructed from the date 12.07.2013 the site was then commissioned into operation from the 30.09.2013. Documentation provided by Alteso (Altesco), reveal the nominal power expected was 27,488,560Wp with an installed capacity of 27,757,999Wp. There are 113,344 Chinese made modules of the type CNBM solar crystalline series II: 235Wp, and 245Wp, that were installed at 30° Tilt angle, Azimuth. There are a total of 50 AEG protect –PV 500 inverters with integrated 25 TKS C1000 making the energy conversions possible.

Several temperature sensors numbered 2, 7, 14 and 25 are located in the region of the study these sensors acquire temperature data from thermometers located on site at the PV plant, wind speed and wind direction is gathered from anemometers (weather station) data, irradiation data is obtained from pyranometers also positioned on site, the system is grounded from lightning strikes and with DC surge protection devices.

Table1: Specifications of PV Plant area

ITEM	UNIT	Value
Nominal Capacity	Wp	27,488,560
Module Area	m²	186,083.65
Module Types	W	CNBM 240W-245W
Dimensions of Module Tables	L*B*H (mm)	1655*992*40
Weight of each table	Kg	19.5
Length of Park	m	189,332
Area of Park	m²	450,000
Arrangement	Landscape oriented rows	4

Data Source: Alteso

2. Climatic conditions of the Region

This information identifies the best season or baseline for harvesting solar energy in this region and provides the basis of the study's window (July- August)

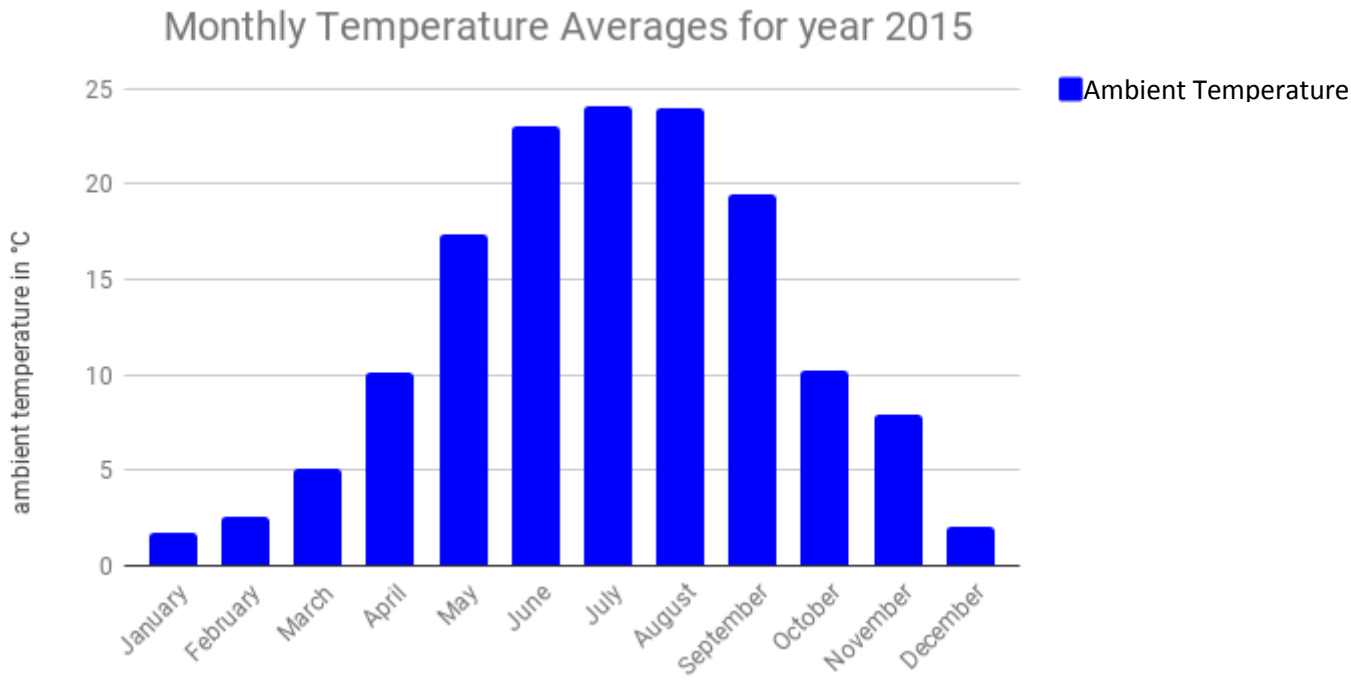

Source: Alteso

Figure 1: Showing average monthly ambient temperatures at PV Plant location

Monthly ambient temperatures for the PV plant under study is shown above in figure1, temperatures are reliably on average above 20°C usually between May and September.

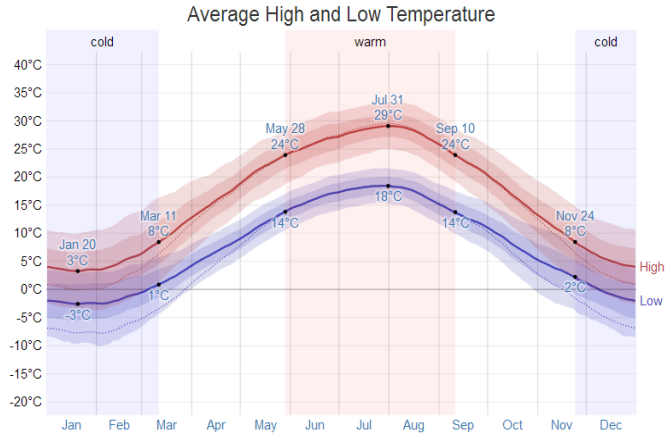

Source: Weatherspark.com

Figure 2: Figure showing Average regional temperatures.

The coldest day of the year is historically January 20. The average range expected on this day is a low of -3°C and high of 3°C as seen above in figure 2.

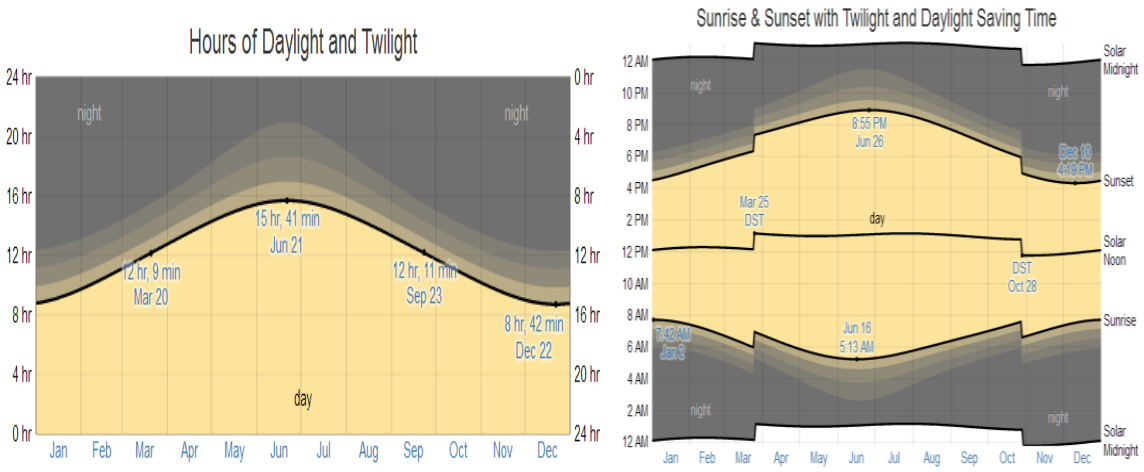

Source : WeatherSpark.com

Figure 3: Figure of Daylight and Twilight in the region.

The visibility of the Sun is demarcated by the black line in the graphs above. Full daylight is represented in orange.

This information gives an idea of availability of sunshine during the days the year considered best for harvesting solar energy as seen in figure 3 above.

2.1 Overview of wind effects

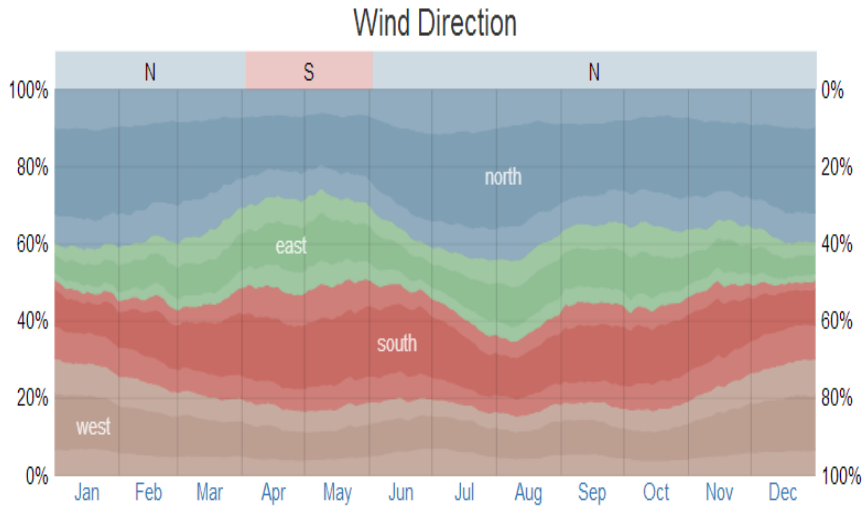

Source: Weatherspark.com

Figure 4: Wind direction averages

In this section an overview of PID, the effects of wind, wind origin (direction) on PV modules are presented in this section.

The hourly average rate and wind vector (speed and direction) as measured at 10 meters above ground is determined by local topography, instantaneous wind speeds and direction will vary more than that of the hourly averages.

The windier part of the year is considered to last between 11th of October to April 24; average wind speeds of more than 4.4meters per second can be experienced.

The wind vector originates most often from the south for 2 months, then from the north for the remaining 10 months. The lightly tinted areas at the boundaries are the percentage of hours spent in intermediate directions (northeast, southeast, south west and northwest). It is thought wind direction plays little to no significance in this study unless it can be proven that the wind passes over a water body before it comes in contact with the site. In addition the proximity from the water body to the site would determine the level of cooling on the modules

The study will focus mainly on the summer periods where production is at its peak and is more reliable than that of the winter period. The comparative changes will be detected and the irradiation values are at their most significant levels during the year.

An excerpt from the initial commissioning report stated under the section titled “O&M influence yield”. “Pollution of the module surfaces, weed and plants casting shadows on the module plain, fractioning or animal bites.” These were all factors expecting to cause a decline in operations as well as strong winds. System losses summed up to a gross 18.1% in the year according to above mentioned report.

2.2 What is Potential Induced Degradation?

Potential induced degradation is a phenomena first seen in the 1970’s and observed in crystalline and non-crystalline modules (Wen and Ross et al.1985, 776), pre existing conditions such as high temperature, humidity and voltage decrease the modules output capacity and efficiency, these losses can be as great as 70%, in some cases physical markers such as corrosion may be visible while others are not. Some effects of PID are reversible, in the case of PID induced by operating at high voltages usually over 100VDC for long periods surface polarization occurs as shown below. If the entire system is negatively grounded, the condition can be remedied if detected early. The effects are more pronounced in large PV installations and will have greater cumulative losses as a result.

PID’s impacts are now more widely known. In one form, the differential between the module frame and the PV cells near the negative pole in a transformer less inverter can cause PID. The voltage differential can become strong enough to cause the migration of positive ions from the glass to the cell itself.

Vulnerability of modules are dependent on various factors such as refractive index and thickness of the anti reflective coating layer, a stacking fault, volume resistivity of the encapsulant (Oh et al 2017, 30 citing Pingel et al 2010, Berghold et al 2010, Naumann et al.2014).Various environmental factors influence the difference in voltage between frame and solar cell according to the string configuration. These are temperature, humidity and solar irradiance.(Oh et al 2017 ,30 citing Hacke 2015a,b).On identification of PID under standard test conditions IEC 62804 a module is considered affected by PID after a 96hr test at 60°C and 85% humidity and power losses of over 5%(Oh 2015 citing IEC TS 62804-1 Edition1.0,2015).

2.3 What is surface polarization in detail?

A negative charge can come from module leakage, accumulating in the silicon nitride which can overcome the positive charge and cause surface potential to move toward depletion or escape, by increasing front surface recombination. The negative charge can come from a

module leaking current while the cells are being operated at a negative charge with respect to the module frame, or ground. There is no Potential Induced Degradation observed when the cells are operated at negative voltage to ground. Modules with back Junction cells are more affected than front junction due to their reliance on front surface passivation. This is reversible with proper grounding (Swanson et al. 2004, 4).

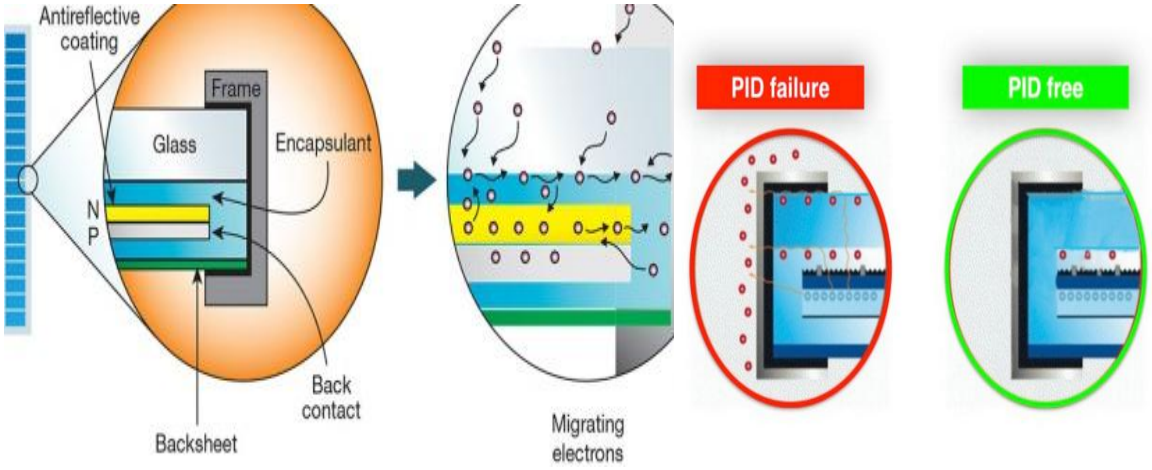

Source: Homepower.com source: solarassetmanagement.eu.com

Figure 5-6: Showing a high voltage potential leading anions (negative ions) into migration, away from semiconductor, instead travelling to the glass package or frame, or to the module's external environment. The phenomenon is more prevalent in hot and humid climates.

The typical voltage at module level is about 30V; the number of panels in series and parallel are then decided. Cells prone to PID have a negative potential. In a typical string, cells have a voltage level of -200V at the negative end and +200V at the positive end. Figure 5-6 illustrates the movement of electrons to in a functioning photovoltaic cell and the migration from the P-n junction is shown in red in the case of cells affected by PID. The electrons escape to the exterior casing of the cell or glass packaging.

2.4 PID Diagnostics in PV power plants

Prediction and early detection hold a particular interest to owners and operators of PV power plants. At system level, a streamlined investigation begins with IR((thermographic) inspection and voltage or I-V curve measurements to identify affected cells of a string of

modules, Plant topology, particularly ground potential and on site electrical layout is evaluated. Local environmental risks are also assessed. The option is always available to remove some of the affected modules for laboratory testing which is costly; this level of testing is performed at Fraunhofer institute for solar energy systems ISE in Germany.

It is not a trivial task correlating indoor testing to outdoor results; outdoor results when available plays a vital role in determining PV performance and lifetime of PV modules. The wealth of Information gained from typical outdoor results is more comparable to large scaled PV production plants.

The most important factor to consider outside of the environmental ones in contributing to the uncertainty in degradation rates is reduced with increases in monitoring time. Regardless of the type of module or the technology, the time of its installation determines the age of the module. Modules manufactured after the year 2000 have exhibited improved stability with time as testing and material efficiency is optimised.

Before PID can be properly diagnosed preliminary testing should be conducted, standard testing has its merits in determining susceptibility. In such tests modules are generally tested under Laboratory conditions, these tests are done for a minimal of 100 hours in the US by NREL, (Lausch et al 2014,) their study states that generally PID susceptibly testing is done in a climate chamber 85°C, 85% relative humidity, -1000V, with only 48 Hour testing time. If successful, modules are deployed to the PV plants for use. The determination of PID‘s existence follows the test procedures outlined below, The electrical procedures aim to determine behaviour of PV arrays and their corresponding inverters.

2.5 Electroluminescence and Photo Luminescence Imaging

This is a very detailed test that is used for discovering if a module presents PID, through electroluminescence imaging of modules with a (CCD) Charge Coupled Device Camera. Luminescence images are acquired by a visible or NIR (near infrared radiation) - sensitive imaging device, which gathers the photons emitted by the radiative inter –band recombinations of the excited charge carriers. When charge carriers are excited by light, the method is called photoluminescence. Where charge carriers are excited by a current applied to the DUT (device under test) it is known as electroluminescence. The module is charged by an external source other than sunlight. The module without the brightness or the luminescence of the others is affected by PID. Electroluminescence image reveals which cells are affected by PID through, darkening or colouration. This is only a visual representation and an indicator of the cells in a module that are shunted by PID, by

extension identification of affected modules in a string is achieved. This method forms the initial step in confirming the presence of PID. In some instances electroluminescence can reveal other hidden defects which had otherwise gone undetected during the quality control phase by the manufacturers.

The recognised tendency is for PID to be located closer to the negative side of the string before gradually making its way to the positive; this test will not indicate how PID affects the site but rather where shunted cells are located. From experiments done by (Pingel et al 2010,3) they have observed that in a floating system, when going from negative to positive, voltage potential increases and degradation stops when voltage potential turns from negative to positive. Differences in temperature indicated by a darker appearance than the surrounding cells, is mostly likely an indication of PID's occurrence, the unaffected cells shows uniform temperature across the module. See figures below.

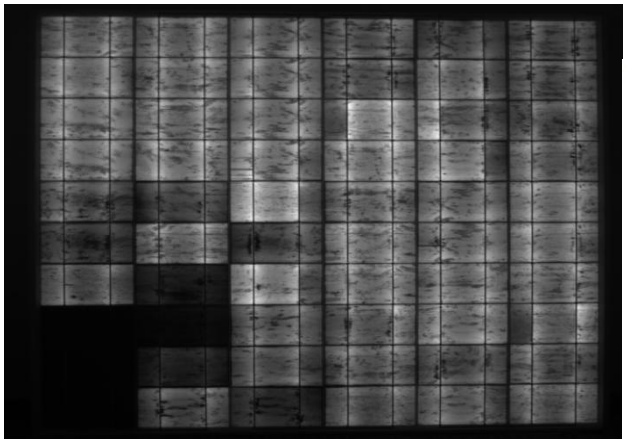

Source: Singh et al 2018,301

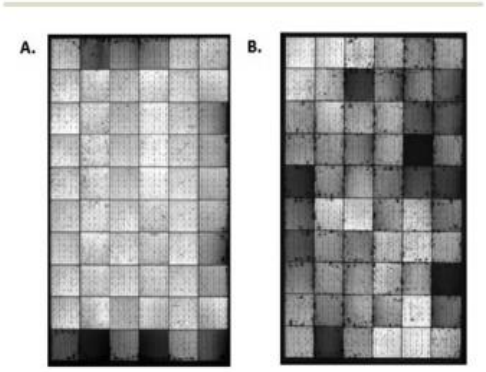

Source: Luo et al 2016, 8

Figure 7-8: Electroluminescence images of silicon Photovoltaic modules after being in a chamber PID test, under high humidity and temperature conditions (A) After a PID test (B) and after with Aluminium foil . The dark cells are shunted or damaged due to PID, it is important to note both modules were in good condition without shunted cells prior to PID testing.

EL image of c-SI PV module, the dark squares are affected by PID.

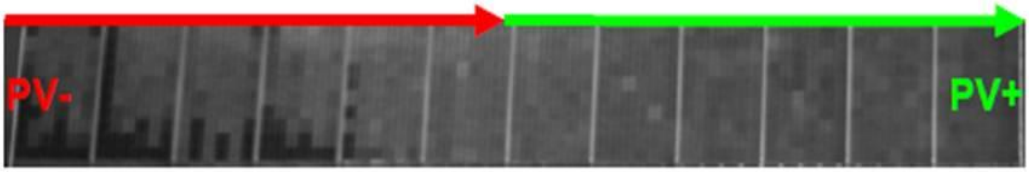

image of a floating PID string with degraded panels on the side with negative potential. Source: POTENTIAL INDUCED DEGRADATION OF SOLAR CELLS AND PANELS; S. Pingel, O. Frank, M. Winkler, S. Daryan, T. Geipel, H. Hoehne and J. Berghold

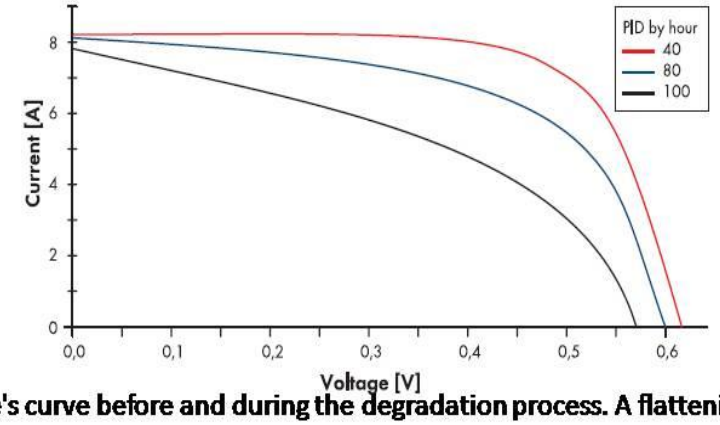

A PV module's curve before and during the degradation process. A flattening of the curve is characteristic, with the open-circuit voltage and the short-circuit current remaining nearly unchanged, and the maximum power point (MPP) being reduced by up to 70%. Source:SMA

Source: S.Pingel et al 2010.Potential induced Degradation of solar cells and panels

Figure 9: EL image and IV curve as Potential Induced degradation progresses across a string.

Daytime photoluminescence (DPL)

This method is contactless and, a non destructive spatial analysis tool for rectification of PV modules. During a field inspection, the modules are excited by the sun's rays, no electrical contacts are required. Its application is used at an early stage of detection for suspicious defective modules in a string. Using a combination of DPL and DEL gives further information about performance losses after imaging analysis.

2.6 Infrared image- forming / Infrared thermography (IR)

Infrared testing is generally done on a sunny day (650W/m²) with an infrared camera, the positioning above strings allows for easier detection of faulty modules or defective cells. It is used is to detect unusual temperature variations in operational modules on site. Overall

temperature will be different to surrounding modules. Thermal stresses may indicate a problem within an individual module or show hotspots, this is indicative of a defective cell or burn marks, which could also cause delimitations in the modules, cells affected by PID which glow red are thought to be hotter than the surrounding cells indicated in yellow. Differences in temperature is the reason for this display, non uniformity across the cell, where one side glows red and the other orange ,yellow or green are colour variations indicating PID's occurrence, the un-affected cells shows uniformity in temperature across the module. As illustrated below:

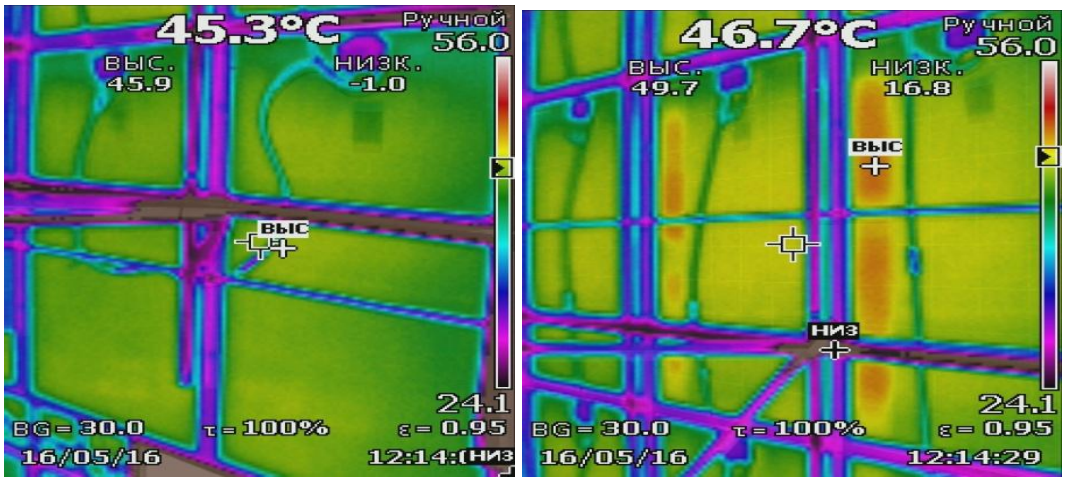

Source: Alteso

Figure10: IR images 16/05/16

The images displayed above are from IR images taken from the unnamed PV Plant, showing differences in temperature across the cells with time, all taken on date the 16/05/2016.

Within seconds of the 14th minute after 12 on 16/05/16, the temperature increased 1.4°C

Temperature is none uniform across the cell, red areas begin to appear in the middle of the cell, where the hottest temperature is indicated as 46.7°C. Progression of non uniform colouration occurs within minutes.

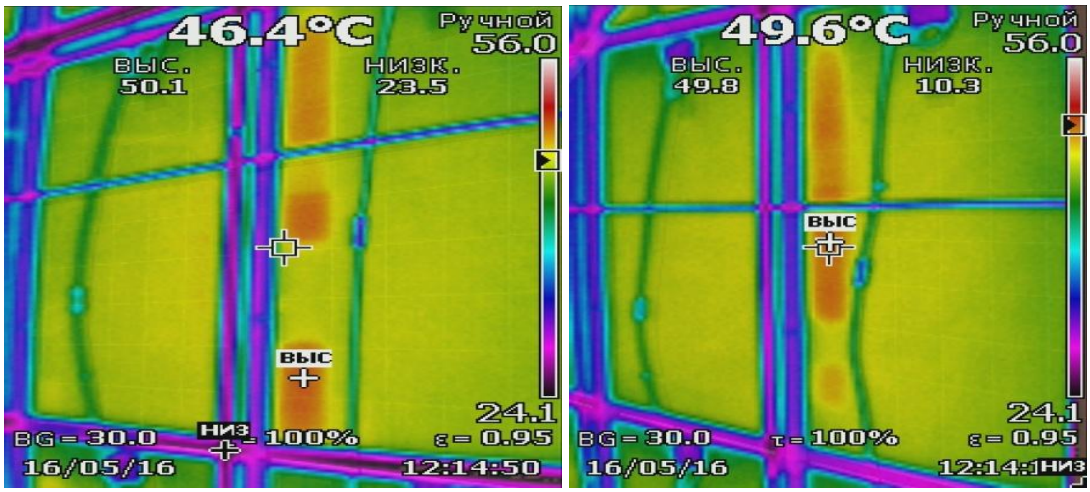

Data Source: Alteso

Figure 11: IR Images from 16/05/16

The images displayed above are IR images taken from the unnamed PV Plant, showing variations in temperature across the cells with time all taken on the 16/05/2016.

Temperature is still increasing from 46.4°C to 49.6°C, 3.2°C, temperature across the cell is remains non- uniform, the red area within the cell also extends north to south, a greater area is affected..

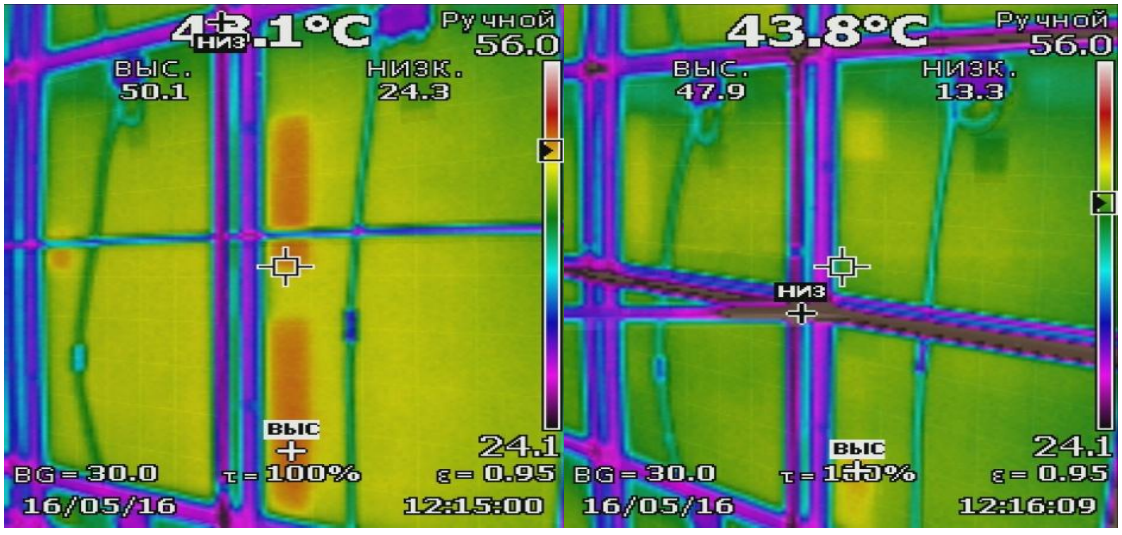

Data Source: Alteso

Figure 12: IR Images from 16/05/16

The images displayed above are IR images taken from the unnamed PV Plant, showing differences in temperature across the cells with time all taken on the 16/05/2016.

After a minute temperature between 12:15pm and 12:16pm begins to decrease from 48.1°C to 43.8°C however the high temperature displayed on the cell is 50.1°C, other red areas appear to the left of cell.

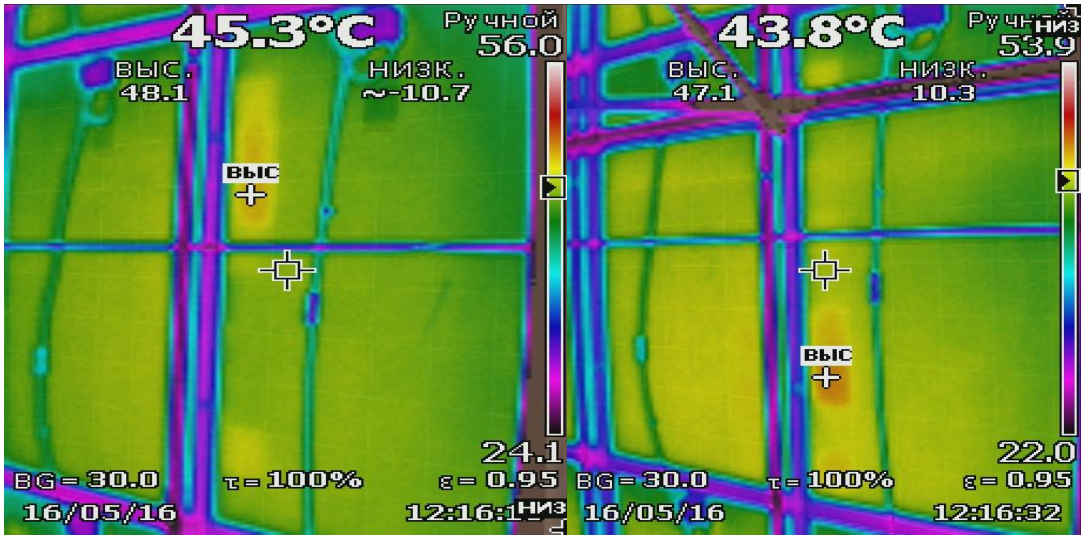

Data Source: Alteso

Figure 13: IR images from 16/05/16

In the 16th minute the temperature continues to fall from 45.3°C to 43.8°C.a 1.5°C difference, red areas are replaced and represented in orange indicating the temp is still higher than the surrounding areas, a non uniform temperature across the module, may be a clear indication of PID, rapid temperature changes in a short time does indicate an irregularity.

These images formed the basis of confirming the suspicion of the owner /operators from a visual standpoint that some form of PID does exist at this site. Uneven temperatures across the modules are clear signs of irregularities, irregularies stemming from low voltage, possible high humidity, cloud cover, dust, shading and or myriad of other factors. These will be further investigated below.

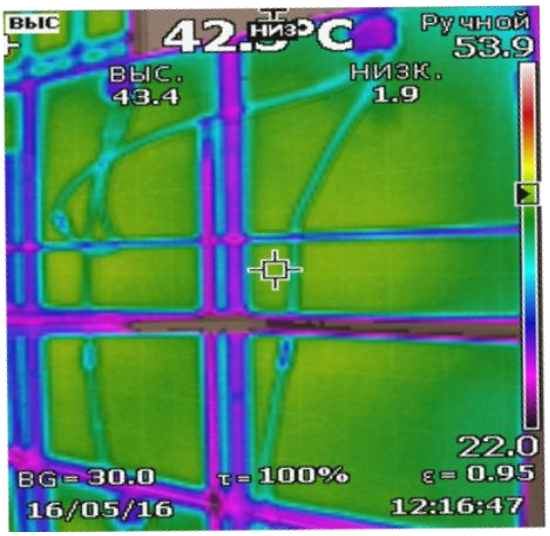

Data Source: Alteso

Figure 14: IR Images from 16/05/16

In under 3 minutes the temperature difference recorded from 46.3 to 42.3 after an increase 49.6°C. an overall difference of 7.9°C in module temperature, non uniform temperature across the cell, with hotspots growing and again decreasing, may well be an indication of irregularites in the form PID.

2.7 Measurement of the PV array

This is a very useful diagnostic tool used for verification, if the array power is coherent with power installed (sum of the power of all the modules). It can be described as a semiconductor diode; the measurement is relatively easy to do. Quantification of performance parameters of PV Panels is essentially what this test is. The detection is apparent when a comparison is made against the manufactures data sheet(or flash- list), it may also indicate if a string is disconnected(burnt fuses, disconnected cables, defects in PV modules) that result is an open circuit condition, this test could indicate aging, premature degradation or other unwanted conditions such as shading and potential induced degradation. A plant operator can potentially build his own IV tracer or purchase one; they are commercially available and specifically designed to measure IV curves. The result of the measurement is a graphical representation of the I-V characteristics within the working conditions.

Measurements of the PV inverter efficiency are usually done simultaneously at input and output to determine compliance with the data sheet, according to the specifications provided by the manufacturer. A simple Wattmeter could be used to perform this testing (Martinez-Moreno ET al.2010, 100) according to Martinez.

Electroluminescence imaging

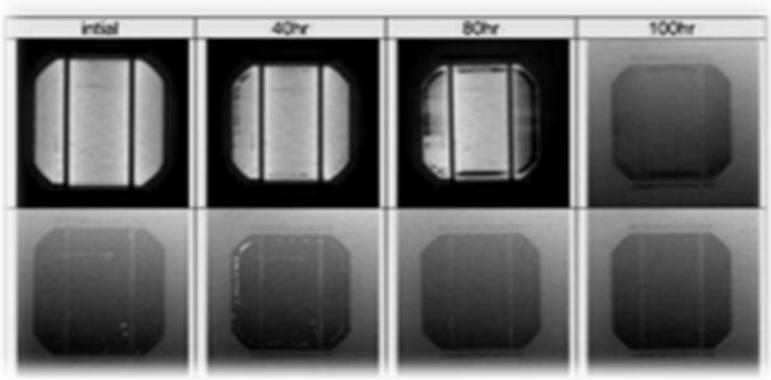

Source: (Luo et al 2016,14)

Figure 15: EL image of a cell during a PID Lab test (Upper row)

Corresponding reverse bias beneath

Open circuit voltage

An initial test for PID is measuring the open circuit voltage with a voltmeter. If the modules are affected by PID, the open circuit voltage is lower than the reference given in the performance sheets.

Operating voltage

This is measured with a voltmeter and more effective at giving information about performance than the open circuit voltage. Affected modules will operate at lower voltages than those unaffected by PID as they are required to deliver the same power as the other solar panels in the string.

Power decrease and current is constant in the other panels of the string, the voltage falls. A fall of the operating voltage is proportional to PID losses.

2.8 IV curves

Ideally the measurements should be made on a sunny day; IV characteristics are measured with an electric tracer, making it possible to observe deviations from the IV curve.

Under IV curves (STC) standard testing conditions is generally an indication of performance of PV modules at specific temperature of 25°C and irradiance value of 1000W/m², air mass 1.5 (AMI.5) spectrum. This is a representation of irradiance and the spectrum of sunlight incident on a clear day on a 37° sun facing , tilted surface at an angle of 41.81° above the horizon. (This condition is representative of solar noon)

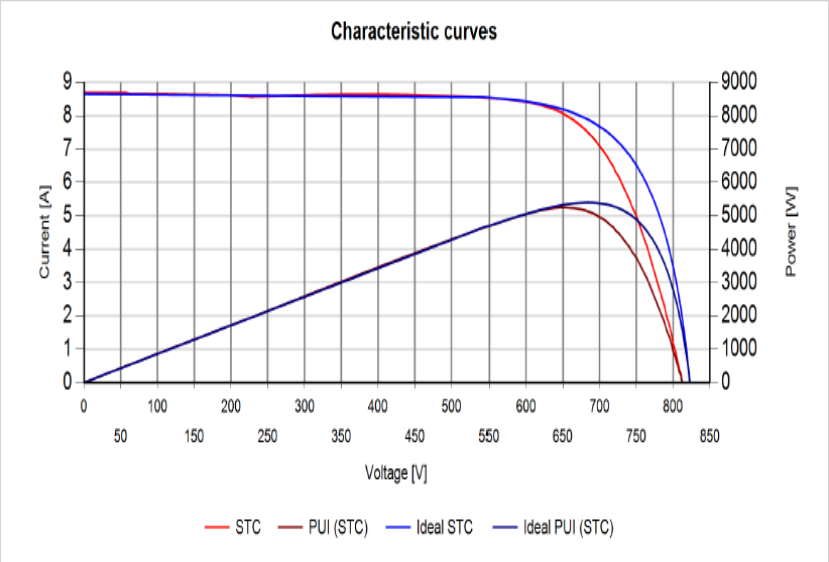

Source: Alteso

Figure 16: Characteristic IV curve

This curve above is from string number 38.05.10 inclination 30°, Power levels recorded show a deviation or characteristics below the ideal or expected output of the modules.

Visual Inspection

A visual inspection is used as a diagnostic tool, its main purpose is to identify and locate visual defects that would affect performance of the PV system. Troubleshooting any mechanical or electrical anomalies, identifying wear and tear on the components where

visible to the naked eye. (Yin Zhang et al.2017.110) Ideally following a checklist, but irrelevant to long term operation of a Large scale PV plant.

3. The effects of wind speed on performance of the modules

Wind Speed has effects on performance from the numerical modelling study of (Siddiqui et al. 2012.3) from these predictions in thermal and electrical performance under varying environmental conditions a loss of between 8.7% and 14% can be experienced with increasing electrical energy.

By increasing wind incidence angle at high velocity (Ceylan et al.2014, 3) found decreases in PV temperature this analysis was done based on the influence of the different ambient temperatures on PV temperature with relation to solar radiation and ambient temperature.

What is seemingly normal is the use of prediction modelling as a method of accurately assessing the efficiency of PV installations. The cooling effect of wind on PV installations and by extension the cooling effect on PV cell temperature was used for prediction modelling, in Bolzano Italy. It is fact that solar panels are solar conductors which make them sensitive to temperature. (C Schwingshackl et al .2013, 77-86) it is necessary to find the physical relation between the PV cell temperature and incoming irradiance and other parameters such as wind and humidity, of these previously mentioned parameters wind is the most influential factor in cell temperature. The most common and standard approach is to model temperature from ambient air and in plane irradiance measurements without the influence of wind being considered on the PV cell temperature. The analysis conducted was at a large PV power plant located in the alpine city Bolzano, Italy over the course of a year between 2011 and 2012. The study contained all the necessary PV technologies of that time to monitor irradiation, ambient temperature and wind speed. From this study it was concluded that wind speed and the inclusion of wind cooling effects played a fundamental role in estimation of PV module temperature. This is recognition of PV cell temperature in determining efficiency of a plant in the absence of cell temperature data. (Hassan et al.2016, 2) confirms that cell temperature decreases efficiency and consequentially electrical power below STC. This means production is greatly affected in the hotter periods of the year when production should be at its highest. Environmental conditions such as high humidity and high temperatures affected performance. Mathematical modelling has been used to demonstrate how environmental factors affect production. From the literature the 21% lower production than the nominal PV conditions could equate to causing monthly energy production losses of up to 10%.

An examination of the rise in temperature between ambient and that of the module will be conducted to determine the effect and or to what extent efficiency of the module is affected. (Hassan et al 2014,4) states that the main reason for module temperature increase is attributable to internal heat generated from the processes involved in absorbed solar energy conversion into electrical energy. Wind has a twofold effect on the modules by increasing the modules angle of incidence at high wind velocity, the modules can be cooled and achieve better efficiency or on the other side threaten the physical components of the systems of a PV plant, the mounting system or the modules themselves. Using numerical models (Kaldelis et al.2014.621) sought to examine temperature and wind speed's impact on module efficiency, their findings confirm operating temperature and wind speed play a crucial role in the conversion process and electrical efficiency and power output are also significantly influenced when thermal energy is released to the atmosphere. The analysis and modelling were conducted under real world conditions and verified on an in situ testing PV Plant.

A modules' power curve is thought to be significantly affected by module temperature. (Schwingschackl et al 2013,76 citing Deutsche Gesellschaft 2010 data) it was found that in these testing scenarios the open-circuit voltage decreases significantly with increasing PV module temperature(-.45%K for crystalline silicon) short circuit current increases slightly ranging from 0.04 and 0.09%K.

Table 2: Standard test Conditions of solar efficiency (STC)

PVC cell Temperature	25°C
Irradiance	1000 W/m²
Air Mass	1.5
Relative Humidity	85%
Wind Speed	1 m/s

The table above illustrates the conditions described as standard test conditions for solar efficiency but these conditions are rarely met or at all exceeded in relation to irradiation in outdoor installations as will be shown below. PV cell temperature is generally accepted to be the temperature of the PV module, however temperature varies across module in the outdoor conditions, there is also variation in a module affected by PID, and temperature across the module is non uniform as evidenced by the IR imaging and thermal imaging. (See chapter 2 above). Solar efficiency and energy yield is greatly affected by temperature.

Analysis of three different PV technologies by (King et al 2002, 1357) found that energy yield is lowered by 2 to 10% at high temperatures. From the study of Schwingschackl into the cooling effect of wind on the PV cell temperature citing (Skoplaki et al 2008), (Koehl et al 2011), (Mattei et al.2006), (Kurtz et al. 2009), They have outlined the importance of wind data for application in their various models showing the importance and impact wind data has in the absence of actual wind data, they attempted extrapolation to determine efficiency on modules. It was (Schwingschakl et al 2013, 7722) concluded the role of wind is relevant for the estimation of PV module temperature and by extension useful for determining module efficiency in outdoor applications.

2014

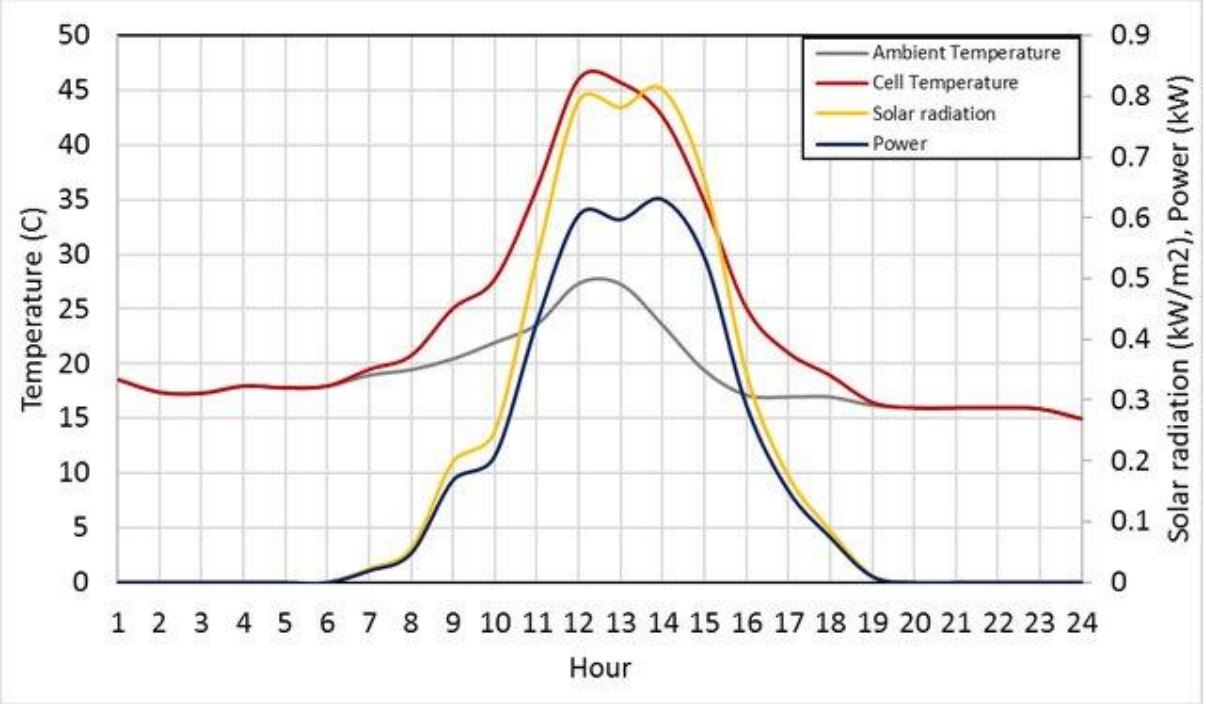

Source (Qusay Hassan et al 2016, 37)

Figure 17: The PV module temperature and electrical power distribution together with model inputs ambient temperature and solar radiation (24th August 2015.) – For a non-tracking system.

(Abass et al.2017,100) have concluded for PV cells to operate at maximum efficiency without energy loss the surfaces need to be clean to allow free entrance of solar photons, pollution dirt and clouds block the sun and have the effect of reducing the ability of generating energy. It would not be an easy feat to measure dust accumulation on the

modules of this site where no mention of a specialised cleaning systems or about the layout which would best indicate dust soiling the modules.

Temperature plays an important role in the correct functionality of PV modules. The modules are tested under standard test conditions(STC) but rarely is on site field testing employed until irregularities are advanced,(Bhattacharya et al 2014,5) investigated effects of Temperature on Photovoltaic module efficiency and concluded that there was in fact some positive correlation between ambient temperature and efficiency this would also play a role in any performance analysis as compared to the correlation between wind speed and efficiency on PV modules. The study was undertaken in Tripura, a hilly area in India. The study made clear that the effects would be lessened on a plain where ambient temperatures would differ to that in comparison, the analysis was done over a 12 month period, it concluded and confirmed that predicting performance of PV modules ambient temperature is a better indicator than that of wind speed, the results achieved may have been regional or site specific as the production levels did not meet the expected desired level of output.

PV cell temperature shows variations under outdoor conditions different to those modelled in a Laboratory. Efficiency and energy yield are impacted by such variations in PV temperature, for example when Temperature reaches 60°C in a free standing system. From statistical analysis values of correlation coefficients are 96% and 68% for ambient temperature and wind speed yields can be reduced by between 2% and 10%.

Photovoltaic cooling has a direct influence on the effeciency of the photvoltaic cells (Hassan et al .2016,2) by extension the capacity to produce electricity. In addition the ambient temperature plays a significant factor during the summer months during the hot period depending on geographical locations

Under (STC) Standard Test Conditions module effeciency is defined at 25°C radiation of 1000 W/m² and a wind speed of 1m/s.This is the baseline or operational standard, temperatures above will not yield STC efficiency and where the inverters are overheating the systems efficiency will decrease, causing power output to shut down. It is known that increasing temeperature decreases voltage and correspondingly electrical efficiency. From Literature models presented for PV temperature the wind speed is not often taken into consideration,it is noted that wind has two effects a positive and negative, the positive effect is to reduce the temperature which increases efficiency, the negative effect comes only at high wind speeds where the physical structures are put through rigidity tests.

The average PV cell temperature for a PV panel without cooling ranges from 33.7°C to 62.1°C ,with cooling the range is reduced to 26.9°C to 34.4°C electrical effeciency from non cooled modules decreased from 7.8% at 200 W/m² to 7.43% at 1000 W/m² but a cooled panel effeciency increased from 8.47% to 10.55% this increase may have been attributed to the irradiation but the uncooled cell does show a clear decrease in efficiency due to increasing temperature, absorbed radiation was observed to be from 200 W/m² to 400W/m², This is applicable in our study it indicates that a cooler module or cell is able to convert energy or absorb irradiation better at high temperatures than that of an uncooled. The finding suggest the system cooling increased efficiency.

It is of note for module validation that there is but a small difference between real module temperature measurement and that of a modelled value , temperature increases has a general negative effect on energy production (during the hot period of a year, significant decreases in energy production was observed to have this undesired effect on the module temperature (power decrease) this was compensated with the power increases on days where temperature was below 20°C. Hot period production is 75%, thermal negative effect cant be fully compensated with power gains this can be seen below.

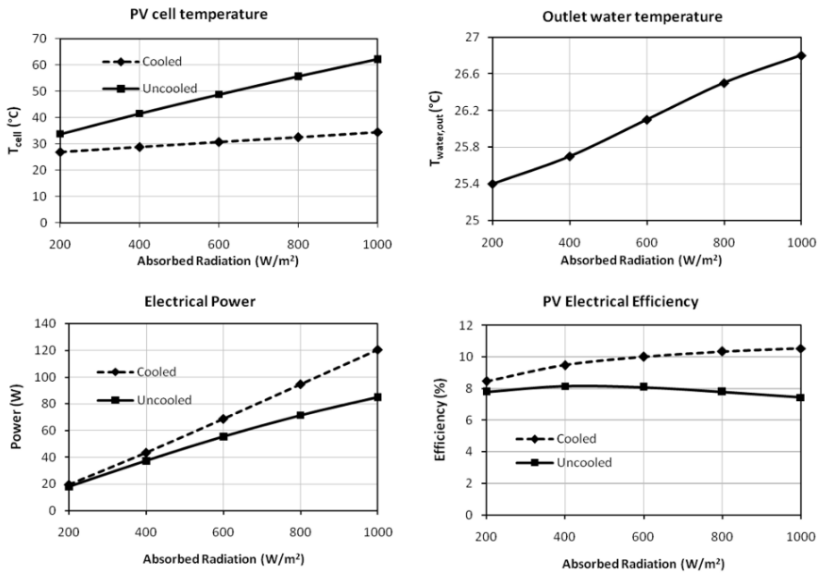

Source: Siddiqui et al 2012.fig12

Figure 18:Cooled vs uncooled modules,power and performance

The adapted figures above from Siddiqui et al 2012 show the differences between a cooled and an un-cooled module and the corresponding electrical efficiencies, it is clear that a cooler module at similar incoming radiation values absorbs irradiation differently than the un-

cooled module, as it is better at converting electrical energy. The difference can be as much 30°C as shown in the PV cell temperature above.

On the site of study, similar temperature differences can be observed between ambient temperature and that of module temperature and it is noticeable from the PV's modules Electrical output or that of the Electrical Power, if we look at the temperature on the 24th of July in the middle of the day it appears the temperature of the modules far exceed that of ambient indicating that instead of converting the irradiation to electrical energy the modules are converting heat energy.

Ambient Temperature also affects PV performance, the models studied accounted for ambient temperatures ranging from 0°C to 50°C. It was noted that without cooling, PV cell temperature increased from 32.5°C to 79.3°C when ambient temperature was between 0°C to 50°C. The electric efficiency dropped by half from 10.46% to 5.16% and the result was that the output also decreased by 50.7%

Examination of the site specific environmental factors, in the absence of humidity data, Wind speed, irradiation, ambient temperature, module Temperature will be assessed as aggravating factors of PID.

3.1 Comparison between irradiation and temperature on an annual basis

For PID's development to be shown, duration of three and a half years of data is presented and should be sufficient to adequately demonstrate a progression. The data provided to the author spans 2015 to March 2018. An analysis of the data with the corresponding environmental parameters will be assessed.

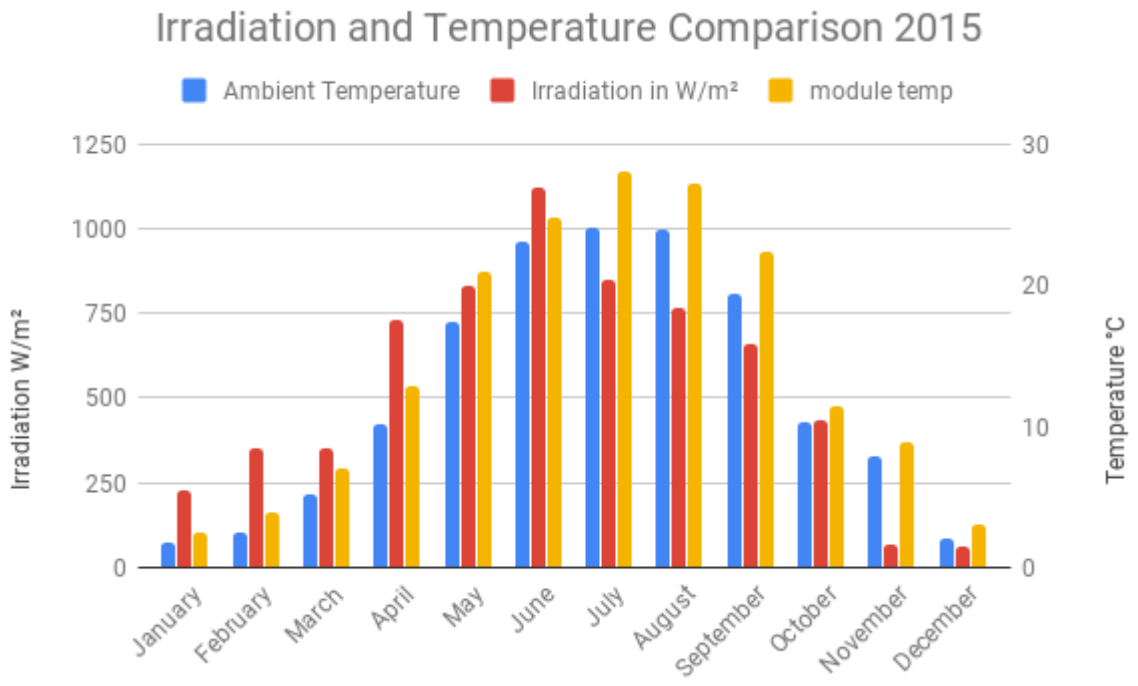

Source: Alteso

Figure 19: Irradiation and Temperature visual comparison for 2015

In comparing irradiation with temperature, for year 2015 above, January measured an average radiation of 229.5 W/m², in comparison ambient temperature was 1.68°C; module temperature is elevated by a degree during this period. Irradiation levels are increased as the seasons change, March shows 349.05 W/m² compared to temperature differential of 1.93°C, April had on average 732 W/m² days whilst temperature climbed to 10.09°C a difference of 2.81°C. June had the highest levels of irradiation on average 1121W/m² with temperatures of 23.07°C ambient and 24.7°C. In comparing the two critical months of July which had 850.6W/m² while August had 768W/m² on average, these irradiation levels were significantly less than in June. High humidity may have played a factor in less direct or diffused radiation being recorded at the pyranometers, June to September from historical records have proven to be the most humid months of the year. This was approximately a year and a half into plant operation. From this wide-angled annual view it can be deduced that module temperature is higher than ambient temperature throughout the 12 month period. regardless of ambient temperature or the season, In the months of July and August the difference in ambient temperature and module temperature are greater than 2°C.This is insignificant during the periods of expected peak production that could indicate the module performance would be affected by high temperature. From the figure above the parameters

represented are averages and not necessarily accurately representative of the day to day operating temperatures experienced at the large PV Plant investigated.

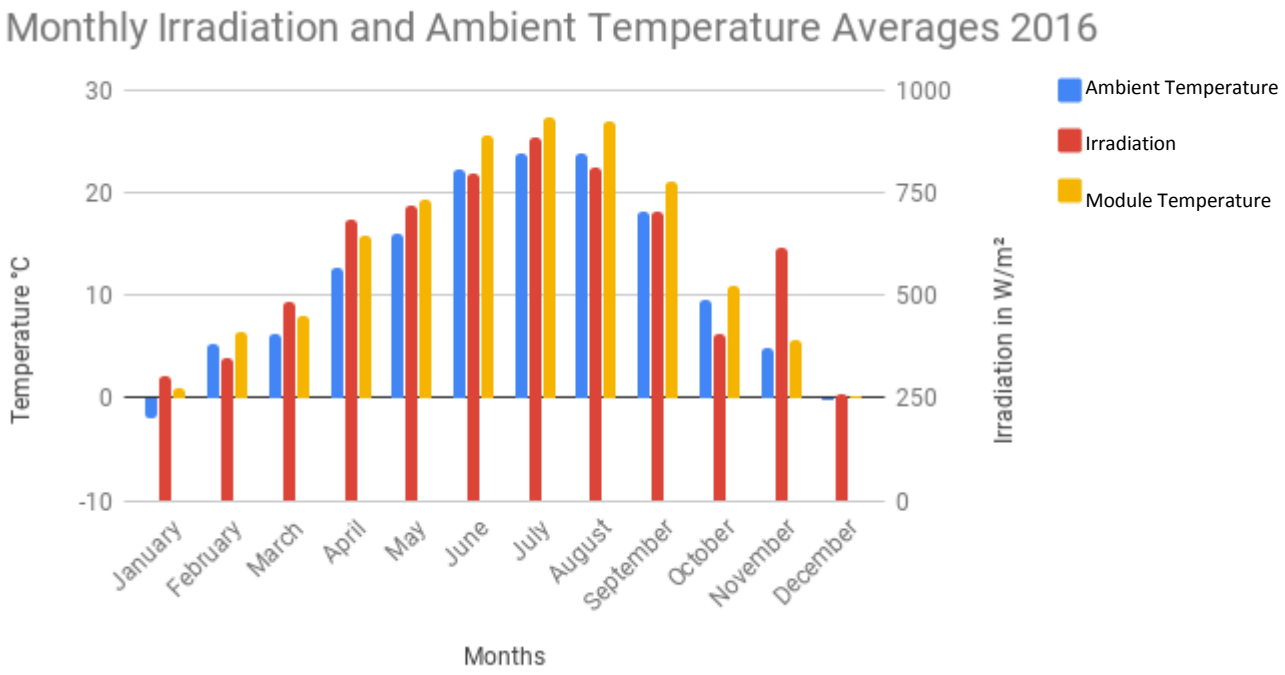

Data Source: Alteso

Figure 20: Monthly Irradiation averages 2016

In 2016 irradiation levels were as expected, lower levels of irradiation in the earlier months of year as seen above in figure 20. January through March due to ever present environmental factors such as higher wind speeds, the possible influence of snowfall and or mostly cloudy conditions which would limit the penetration of direct radiation reaching the modules. Irradiation levels measured by the pyranometers record on average 485W/m² of irradiation in March, April had 686 W/m² a difference of 3.0°C. A module temperature of 15.7°C and ambient temperature of 12.7°C was later recorded, May had 240W/m² and a difference of 3.4°C between ambient and module temperature, in June irradiation averages were slightly higher at 796W/m² the temperature difference was .1 of a degree higher than in June, 25.6°C on the modules and 22.1°C ambient temperature, in July the difference was .2 degrees in difference module temperature was 27.4°C and 23.7°C ambient temperature. Measured irradiation was as high as 885 W/m². In August the difference in average grew to .7°C. Possible explanations for these variations may be as follows: Irradiation levels are higher than that of the previous year 2015, which would indicate expected higher levels of

production for that year, its apparent July and August have the highest levels of irradiation and the highest average module and ambient temperatures during the year, but it also appears irradiation was also high in November. This could be accounted for by diffuse radiation or early snowfall, at face value the levels recorded could be misleading and another explanation may require a closer inspection of November 2016 data, for the purposes of this study it will be excluded as this is not within the peak production period of the study.

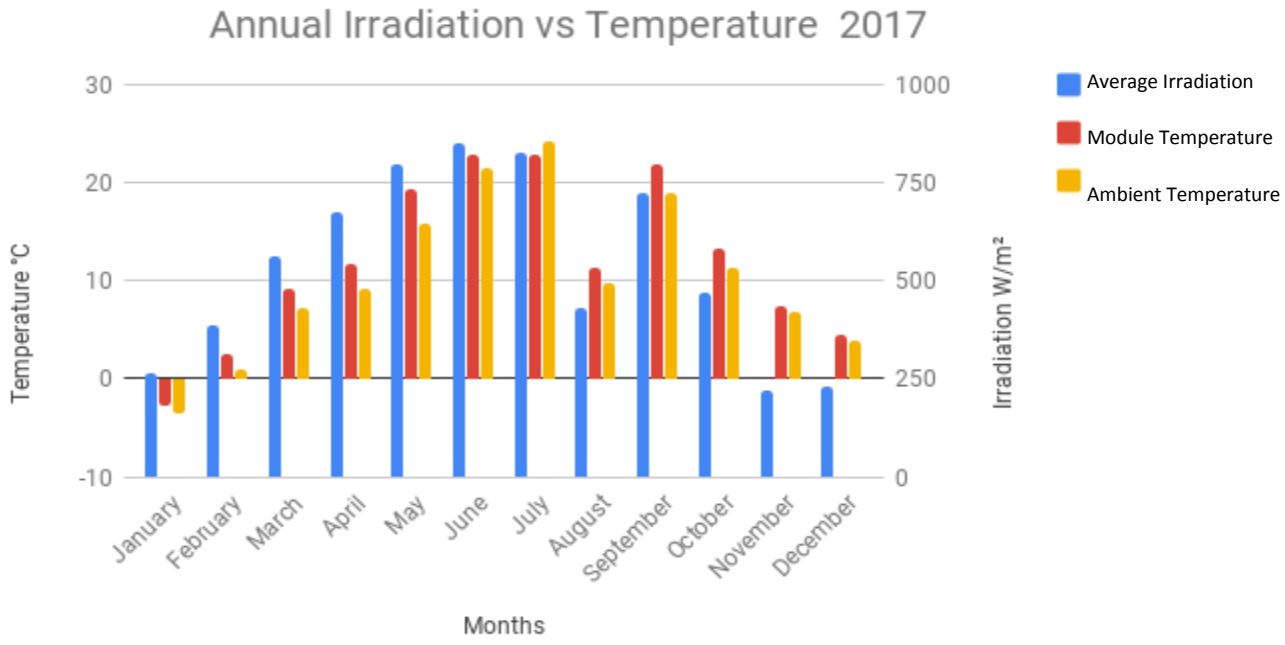

Source data: Alteso

Figure 21: Annual Irradiation levels for 2017

An Overview of Irradiation levels for the year 2017 is shown above

Table 3: showing average monthly Temperature and Irradiation values for 2017.

Summary table	2017		
Months	Irradiation in W/m²	Ambient Temp.°C	Module temp average °C
January	264	-3.5	-2.8
February	385	1.0	2.5
March	562	7.1	9.1
April	673	9.1	11.7
May	795	15.9	19.4
June	850	21.4	22.8
July	824	24.21	22.8
August	428	9.8	11.3
September	722	18.9	21.7
October	468	11.4	13.1
November	220	6.75	7.4
December	229	3.8	4.4

Data Source: Alteso

In 2017, from the figure 21 and table 3 above, it is apparent that the first quarter of the year progressed as the first two previous years, with lower levels of irradiation in the first quarter. In June irradiation was 850W/m² which is within a similar range as that of the two preceding years with 22.82°C ambient temperature 21.48°C on average. July had 824 W/m² with module temperatures on average of 22.8°C and ambient temperature 24.21°C being higher on average. This is the first time this has occurred since 2015. Irradiation levels are higher than the previous year, from as early as March of 2017 in comparison to 2016. September had lower levels of irradiation than the previous year. The average ambient temperatures are generally higher than ambient.

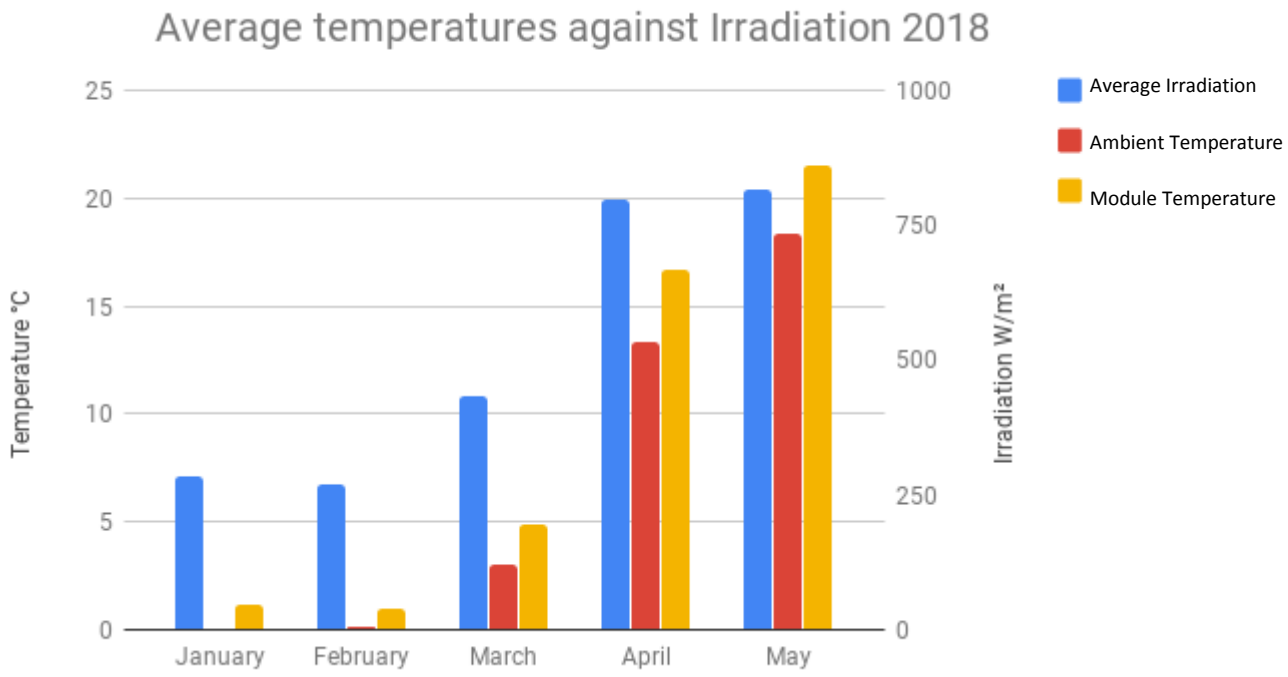

Data Source: Alteso

Figure 22: Average Temperature Plotted against Irradiation for 2018 (Jan –May)

For 2018, seen above in Figure 22, it is observed that the general trend of the previous 3 years has been followed. generally low radiation levels in the earlier part of the year due to snow or cloudy conditions, in March irradiation improves on average and correspondingly ambient and module temperature also rose. May shows increased levels of radiation but raises no alarms about extremely high temperature reading on average which would render the performance of the modules non-productive from the perspective of the effects of PID.

3.2 Comparison of Wind effects on average Temperature

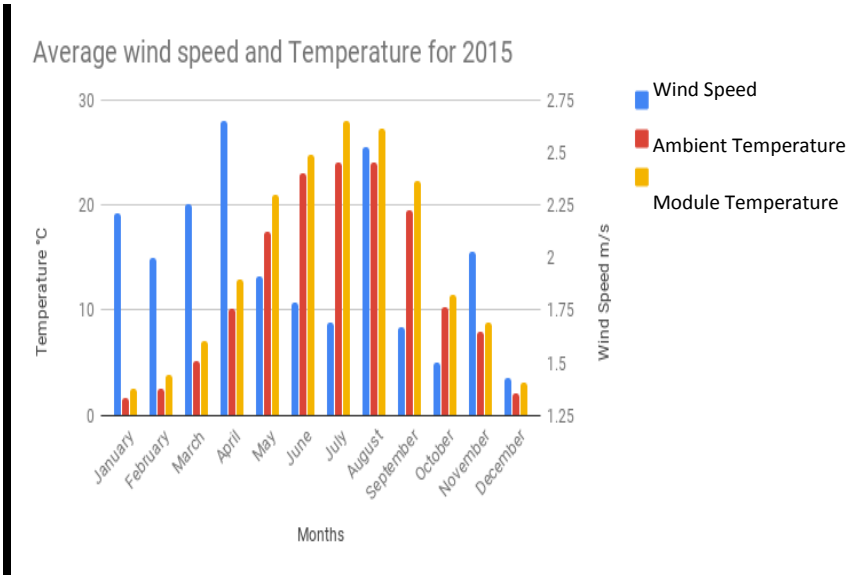

Data source Alteso

Figure 23: Comparison of Temperature (ambient, module) and wind speed for 2015

In figure 23 above a comparison of wind speed is matched against temperature for both ambient and module temperatures in 2015, for most of January to March, the winter months had high wind speeds with the highest wind speed averages recorded in April with 2.6m/s leading up to June where wind speeds did little to impact temperature change in May. The difference between module temperature and ambient temperature was 3.6 °C with wind speeds of 1.6 m/s. Temperature difference was 3.98° C and in August wind on average was 2.5 m/s but temperature difference was still as big 3.2 °C .This wind speeds at 2m/s and below are seemingly insignificant to influence a temperature change in the modules, from the literature wind speeds exceeding 5m/s would be of note in disrupting the module. In June Temperatures averaged 23°C while wind speed averaged 1.9m/s, July averaged 24°C compared to 1.18m/s wind speeds and August recorded 24°C on average, wind speed of 2.6 m/s, September Averaged 19C with wind speed being 1.8m/s. Average temperatures are higher in May, June and July hovering under 25°C while wind speeds on average were

decreasing until August where average wind speeds increased to 2.8m/s, the correlation between wind speed and temperature of modules. (Qusay et al.2016 citing Armstrong et al.2010) observed thermal behaviour of three Photovoltaic modules at different wind speeds (0.77, 2.14, 5.76m/s) they concluded that there was a parasitic difference between convective and radiative heat loss from the modules at different wind speeds. (see also Schwingshackl et al 2013) after testing revealed temperature as a function of solar irradiance, ambient temperature and wind speed, making necessary the inclusion of wind cooling effects in their estimations. From the figures above, this cooling effect of wind on the modules at these wind speeds are not immediately clear, the difference in temperature between August and July is merely 0.18°C where as wind speed difference was on average 0.9m/s between the two months. Module temperature on average saw a difference of 1°C. This may be indicative of the cooling effect of wind but in this region on these facts then it remains difficult to clearly see the exact correlation between the two parameters.

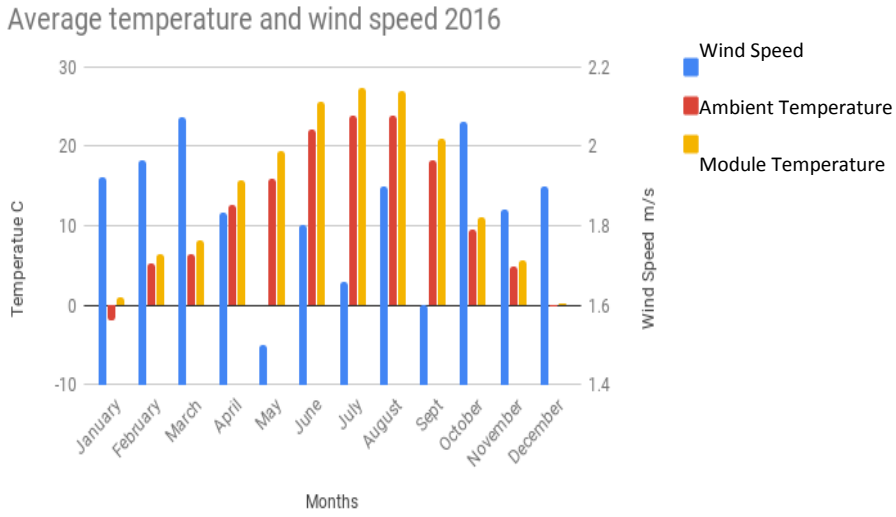

Source Alteso

Figure 24: Comparison of Temperature (ambient, module) and wind speed for 2016

From figure 24 above, we can deduce January through March were the windiest months with average wind speeds ranging from 1.9m/s to 2.0 m/s in March in comparison these being cold winter months where average ambient temperature was on average below 0°C wand module temperature was just above 0. October was one of the windiest months on average in 2016 with a 2.1m/s, but October had 2.19m/s wind on average. Proceeded by

January and February which are colder months, with less direct radiation but a greater abundance of reflective radiation. Provided that there had been some snow fall and minimal cloud cover. However January through March historically has seen a 39 to 45% chance of having mostly cloudy skies or 13-21mm liquid equivalent snowfall. Average ambient temperatures increased from 14°C to 20°C leading into spring. In October wind speed on average was 2.06m/s but the difference between module temperature and ambient for March and October were similar. Wind speed averages were 1.55m/s and 1.77m/s second respectively. This is no cause for alarm as average temperature for the month of October was 9°C well in operating range of the modules. October is noted as being cold and ambient temperatures would be naturally cold in any case, examining the months of June ,July and August which had wind speeds averages of 1.8,1.6,1.9m/s,. The most significant difference in ambient and module temperature was recorded in July with 3.62°C it would be difficult to attribute this high difference to the lack of wind travelling over the modules, even as the other two months preceding and following recorded less temperature differences than that of July. The modules are more susceptible to the effects of high heat in summer, it is likely a wind speed of 1.5m/s could decrease temperature at the site but not significantly. These relatively small temperature changes do not indicate any symptoms of PID, average temperature has not exceeded 25°C. The years following this may prove or disprove this premise, in this study, if wind speed plays a factor in cell temperature.

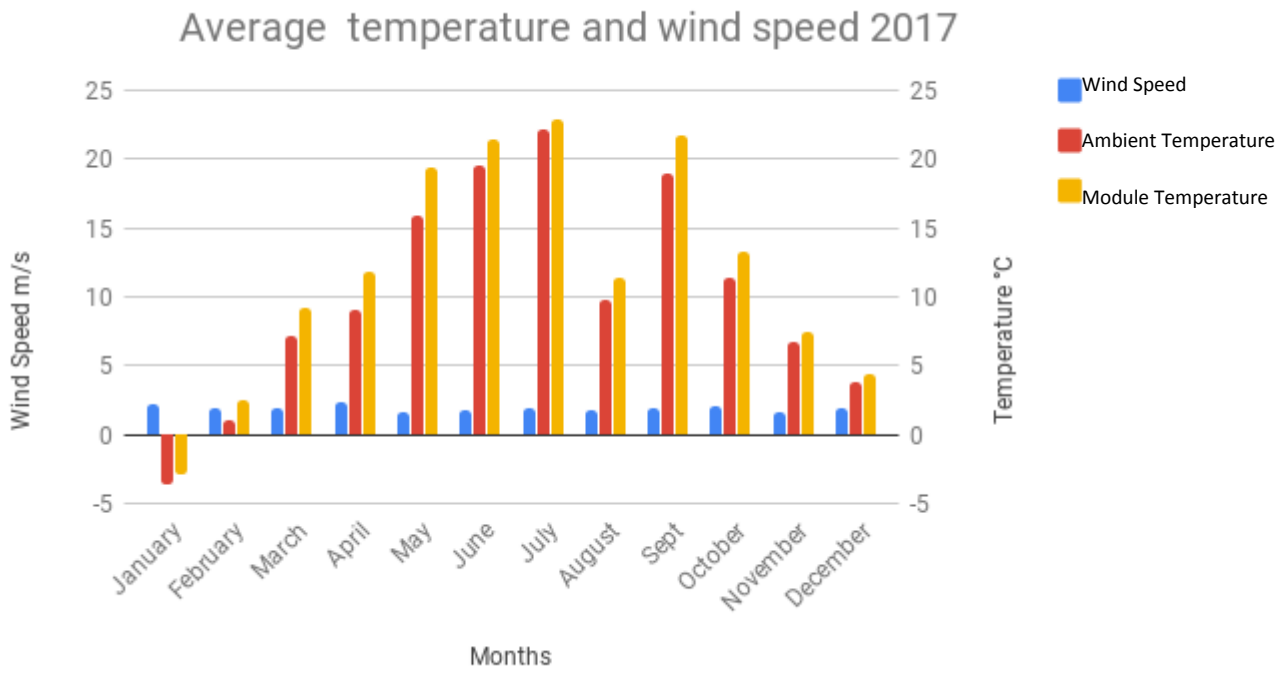

Source Alteso

Figure 25: Comparison of average wind speeds for 2017

From the figure above in comparing wind speeds to temperature, the patterns are similar to that of 2016 higher average wind speeds are experienced in the 2017, June had a difference of 2°C between ambient temperature and module temperature, wind speed was 1.7m/s in comparison to the previous year when temperature difference was bigger at 3°C.More interestingly May had a greater temperature difference of 3.5°C. July however has a temperature difference of 0.61°C at wind speeds of 1.8m/s and August at 1.58°C higher at 1.8m/s wind speed. August of 2017 proved to be less hot than that of the previous year 11.3°C was the average module temperature, and ambient temperature of 9.8°C, July had average wind speeds of 1.8m/s but temperatures soared to a high of 22.2°C on average and module temperature was recorded 22.8°C. The observation is that between July and August similar wind speed are seen without the exact influence of heat from the Sun. August had higher differential temperatures than that of July. This has not given credence to the fact that module temperature is being reduced or cooled by wind. Assuming it was the case, the cooling effect is not immediately visible from the figures above. Temperature fluctuations are a daily occurrence and module temperature is usually 1 or two degrees higher than ambient, the lesser the difference in degrees could be explained as the influence of wind as a cooling factor.

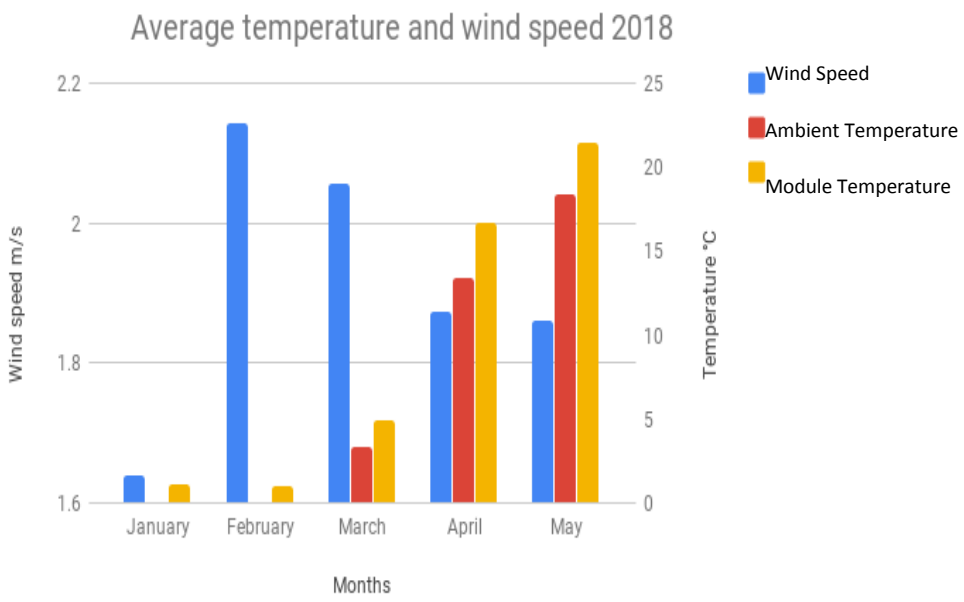

Source Alteso

Figure 26: Comparison of average wind speeds for 2018

There is no significant difference experienced in the first quarter of 2018, in March the differentials in module temperature and ambient temperature is 1.6 °C, while in April its 3.3°C and May 3.1°C. At no point over the course of this 3 year 5 month duration has module temperature been less than ambient especially during the summer months, whether wind speeds onsite are 1.3 m/s or 1.8 m/s the result has been that module temperature is between 1 and 3 degrees above ambient temperature, this seems contrary to the literature, but other factors that have may contributed to this is likely the influence of irradiation absorbed by the modules and converted to heat energy.

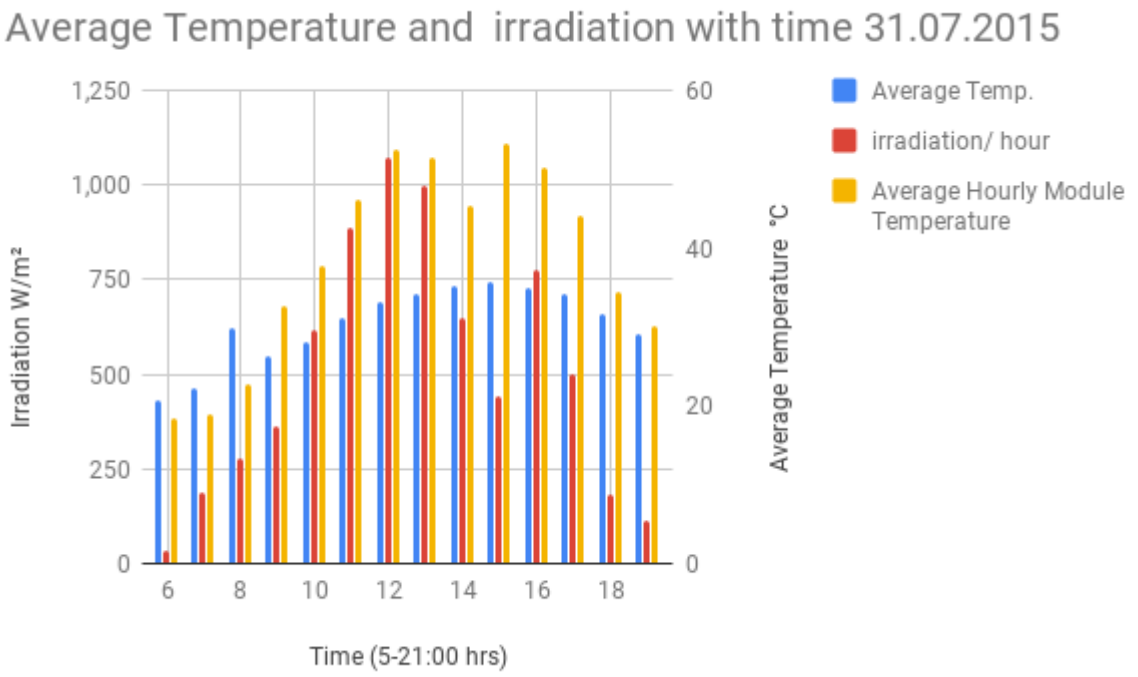

Source Alteso

Figure 27: Comparison of average temperature with time

From figure 27 displayed above for the date 31.07.2015 a greater level of visibility is apparent. Progression of temperature is more visible, it is important to note that irradiation is represented in W/m² and over the course of a 15 hour day. At 8 a.m. Ambient temperature is 30° C in comparison to module temperature being lower at 22.8°C from annual graphs and monthly graphs this isn't visible, the progression of temperature continues into 9a.m when ambient average temperature is 24°C and module temperature jumps to 32.8°C. At 10a.m the situation becomes worse as temperature rises to a 28°C while module temperature is 9°C higher than ambient at 37.8°C irradiation was at this time measured at 918W/m². At 11 am module temperature is at 46.1°C a difference of 15 °C between module temperature and ambient while irradiation levels are measured at 888 W/m².

At midday 19°C is the difference between the two temperatures. Temperature module Temperature is 52°C and ambient is 33°C. Temperature then decreases after 2 pm with a difference of 17.3°C, at 3p.m. the difference is reduced. At 5 pm. the difference is 1.1 °C with average temperature being 29°C and average module temperature being 30.1°C.

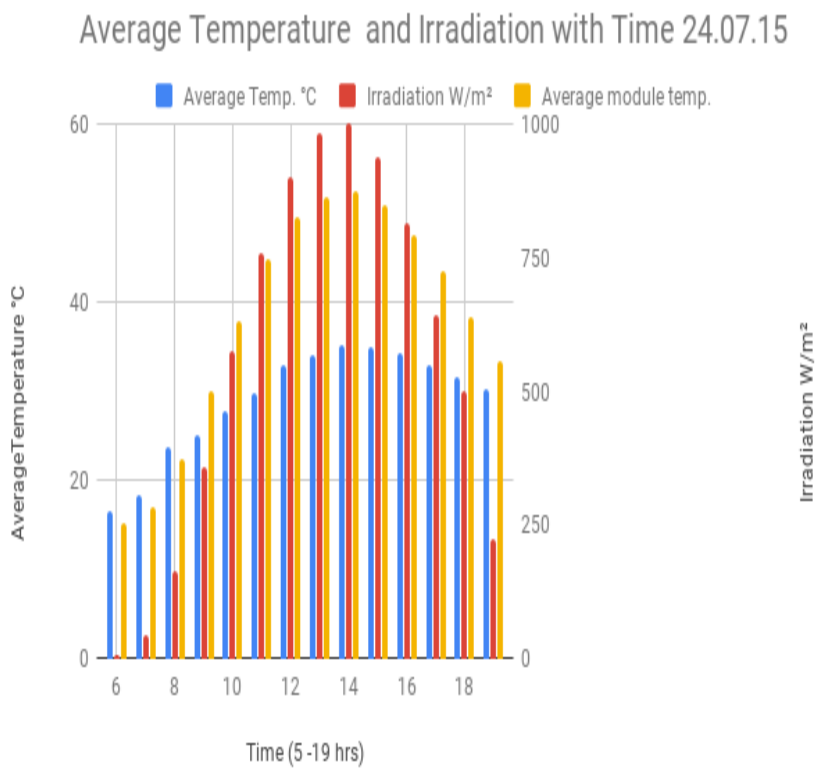

Data Source Alteso

Figure 28: Short term comparison of average temperature with time for 24th July 2015.

The figure above shows the average temperature and irradiation over the course of the historically hottest day of the year in this region, with 30° Tilt angle on the module tables the highest levels of radiation was recorded at midday when the sun is expectedly positioned nearly vertically above the modules and less possibility of shading is occurring , no wind, little to no cloud cover is thought to be diffusing the radiation going to the modules, average ambient temperature is generally lower than that of the modules but at midday it appears average hourly module temperature was 7°C higher than Ambient,

The highest measured levels of irradiation was at mid day at 1072 W/m² .One week later, the 07/08/2015, temperatures rose similarly to that previous week, at 6 a.m. a difference of 1°C was observed between module and ambient, with ambient being the lower of the two temperatures, as irradiation increased so too did ambient and module temperature at 11a.m. with 888W/m² irradiation, the greatest difference in ambient temperature and module

temperature was15°C and thereafter decreasing as irradiation levels also decreased, the ambient temperature and module temperature remained high at 29°C and module temperature at measured at 26°C which is just above optimum efficiency temperature.

The behaviour of string numbered 35.03.02 (PID affected) between the hours of 10 and 15, shows production is less than its two nearest strings, its production is generally slower than that of the neighbouring strings 35.03.03 and 35.03.04, this could indicate little or no wind interference or limited cloud cover, the losses are detailed below.

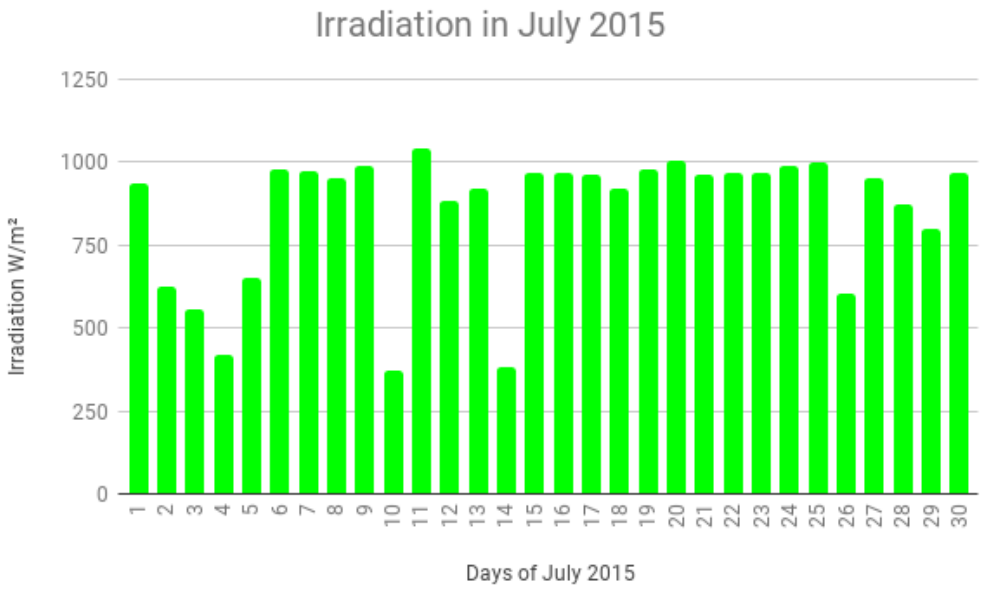

Data Source: Alteso

Figure 29: Daily average Irradiation values for July 2015

In examining the dates of July for 2015 with similar Irradiation values days 20 and 25 can be clearly distinguished above.

Table 4: Shows a summary of percentage losses on days of comparably high average irradiation values for July 2015.

July 2015	Irradiation value W/m²	Red vs. Brown % difference in production	Red vs. yellow % difference in production	Brown vs. yellow % difference in production
Day 20	1,005	4.1% difference	4.1%	0.2%
Day 25	999.9	0.2%	0.6%	0.63%

Data Source: Alteso

It is evidenced in the table above, the at the end of the month with higher irradiation values losses tend to be lower in 2015 between the known PID affected string and strings labelled brown and yellow, the losses were similar on average, percentage wise, but later reduced on day 25. The losses are calculated by differences in production between good and bad strings and expressed as percentages. See table 4 for comparisons.

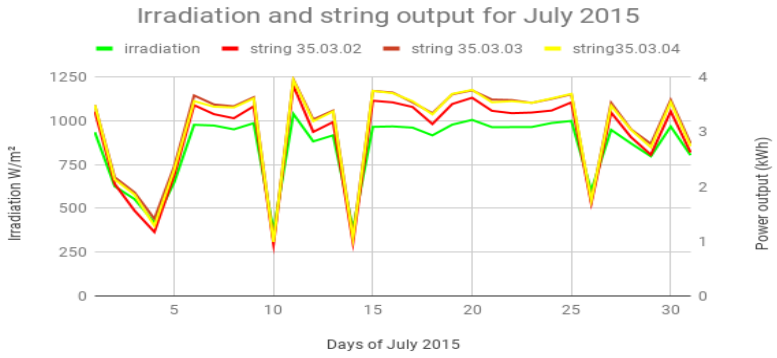

Source: Alteso

Figure 30: Irradiation plotted against string output July 2015

The general trend in performance follows that of incoming irradiation. A direct relation can be witnessed between output and measured irradiation. Variations in string performance are also visible, with most noticeably string numbered 35.03.02 (PID affected) underperforming

in output to the neighbouring reference strings.

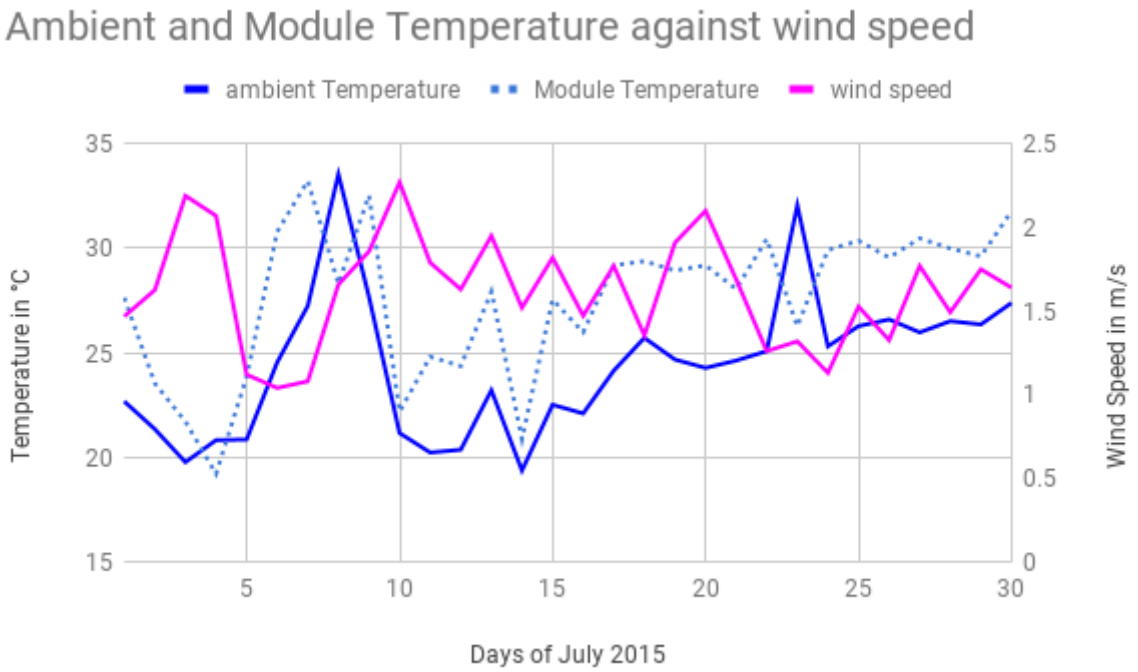

Data Source: Alteso

Figure 31: Temperature against wind speed July 2015

In July 2015, its appears that module temperature is in general higher than ambient and directly proportional to wind speed, with higher wind speeds in the first few days of the month. Average wind speeds of 2m/s result in temperatures below 25°C in ambient and module temperature after day 5 .It can be observed that there is an inversion of temperature and wind speed, low wind speeds under 1.2m/s results in temperatures above 33°C, Temperature in July of 2015 is inversely proportional to wind speed.

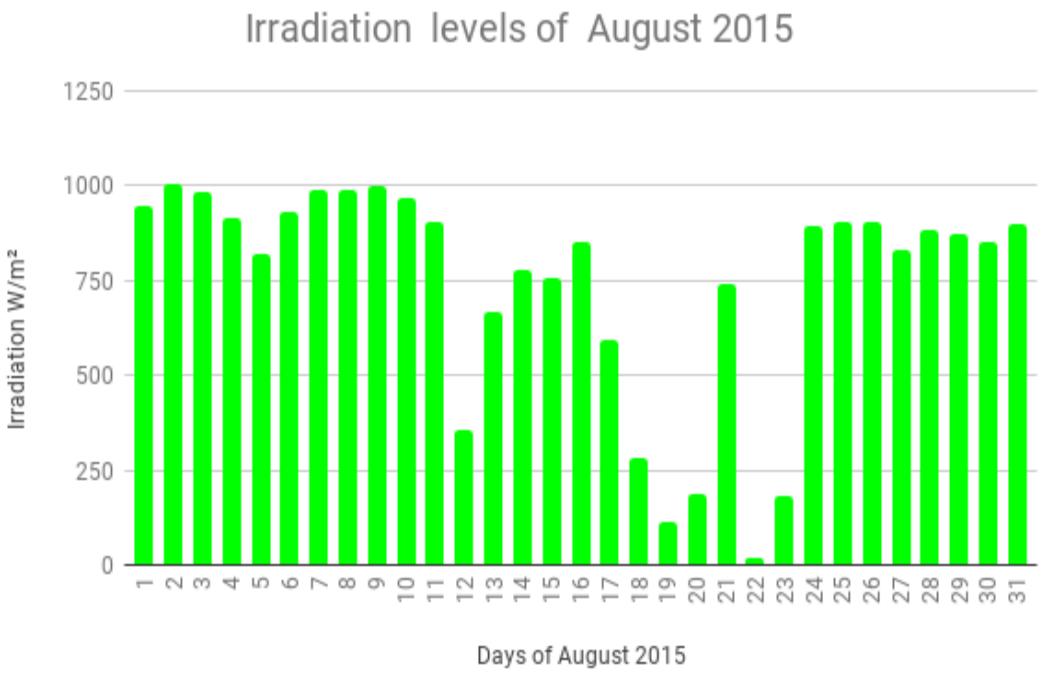

Data Source Alteso

Figure 32: Irradiation levels for August 2015

Irradiation levels for August 2015 are shown above and explained below in table 5 and the text following. Higher levels of Irradiation are experienced first half of the month.

Table 5: Shows a summary of average losses in the month of August on Days of comparable irradiation.

August 2015	Irradiation value W/m²	Red vs. Brown %	Red vs. yellow	Brown vs. yellow
Day 4	915.42	6.3% diff	2.7%	3.7%
Day 11	906.3	5.5%	1.8%	3.7%

Data Source Alteso

In July 2015, it's evident that the PID infected string (red35.03.02) is performing erratically, average differences are noted above, however the average differences between the references are the same on both days but varying between the red/ brown comparison and the red yellow comparison day 4 having a slightly higher average in irradiation had also a

higher percentage differences in performance losses. Losses are increasing over time on the named strings.

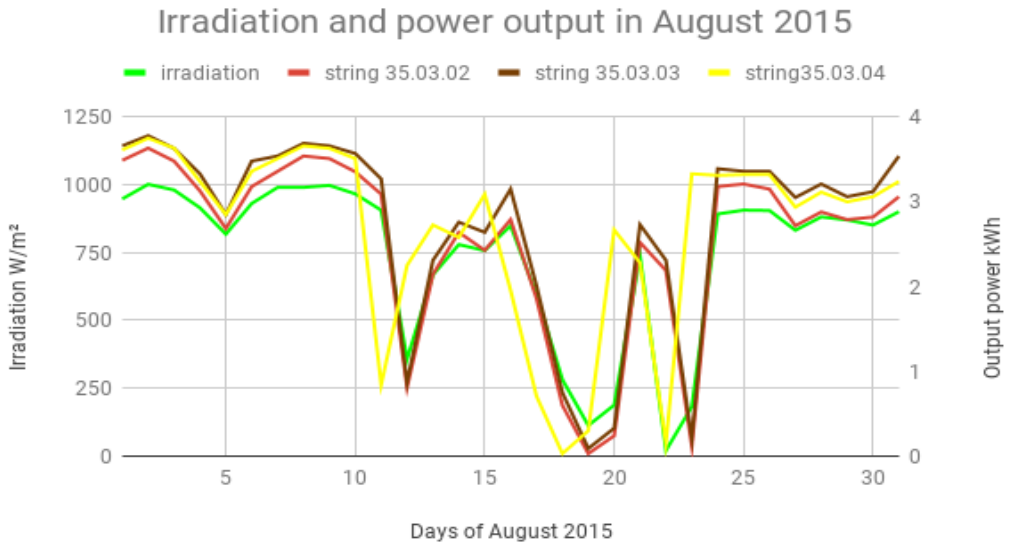

Source Alteso

Figure 33: Irradiation against output for August 2015

The strings of reference and the affected string identified as red in all tables react to the direct and indirect irradiation measured at the pyranometers, reference string in yellow appears to pre-empt, (shifted forward) the pattern of irradiation Day 11 through day 19, inspection of the patterns show the red labelled string consistently underperforming its neighbours.

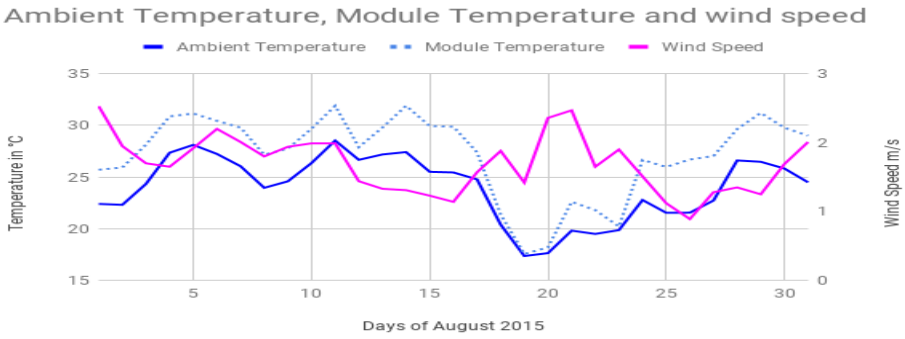

Source: Alteso

Figure 34: Temperature and wind speed for August 2015

In August of 2015, seen above, visibility of the effects of wind speed on temperature are less evident on days 4,11,16,26 , wind speeds of 2m/s or higher produce little visible change in ambient temperature and module temperature remains almost consistently in the range of 4° higher than ambient temperature, throughout the month. Inverse proportionality is shown above between ambient temperature and wind speed; this is conformation of the referenced literature, between days 5-10 and days 17 through 24.

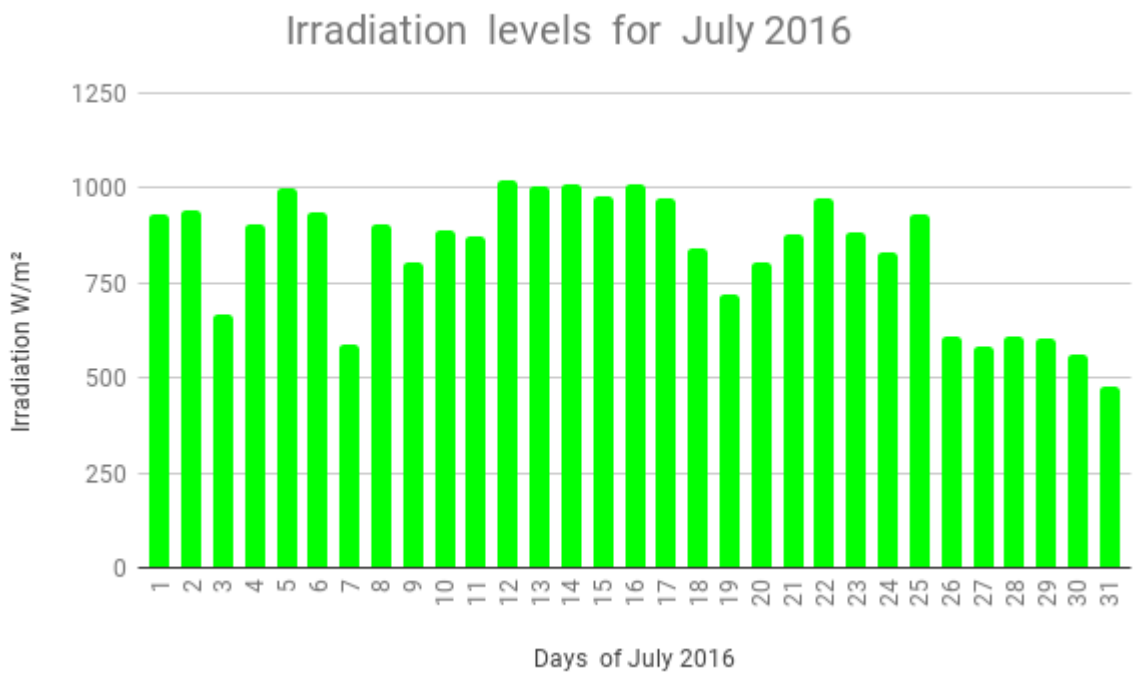

Source: Alteso

Figure 35: Irradiation levels for July 2016

See above figure for irradiation values 2016, explanations follows below. The middle of the month appears to have the highest levels of radiation.

Table 6: Comparable days of irradiation for July 2016 with losses expressed as percentages.

July 2016	Irradiation value W/m²	Red vs. Brown %	Red vs. Yellow%	Brown vs. yellow
Day 2	938.82	7.1% diff	2.5%	4.7%
Day 6	933.72	4.4%	1..7%	2.7%

Data Source: Alteso

Variations are observed in the level of the losses experienced in July 2016 Table 6, as evidenced above between the two comparable days of average radiation levels of 933.72 W/m² and above, it is evident that higher radiation levels earlier in the month produces greater losses on the PID String when compared to that of its neighbouring brown labelled string or yellow. The losses experienced are comparisons between the reference strings and the PID infected strings f (red 35.03.02) for day two and six and shown in table six above and expressed as percentages

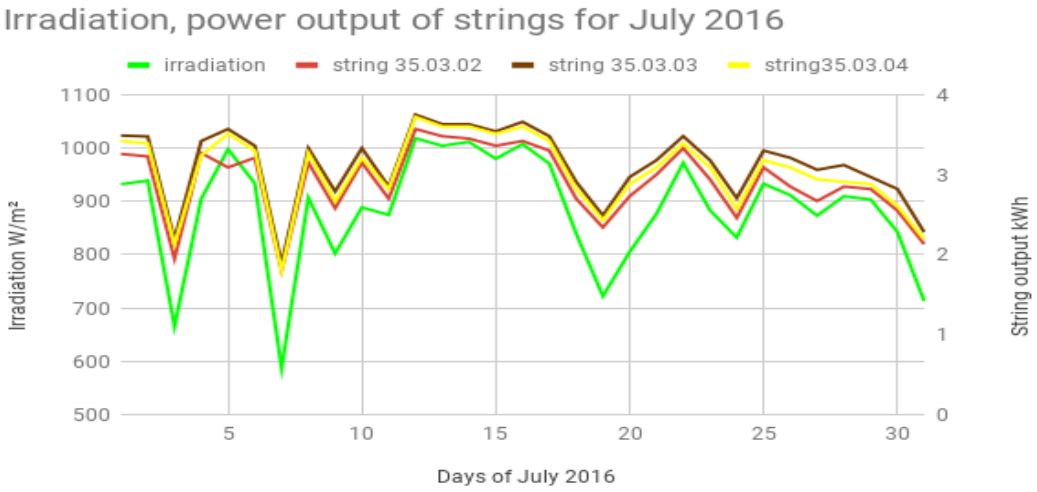

Source: Alteso

Figure 36: Irradiation plotted against output July 2016

From the Figure 36 above the trend of power output follows that of measured radiation levels above indicated by the green line, reference strings coloured in brown and yellow mirror each other, the yellow string is consistently below the brown but more significantly, the PID affected string performs visibly below the references.

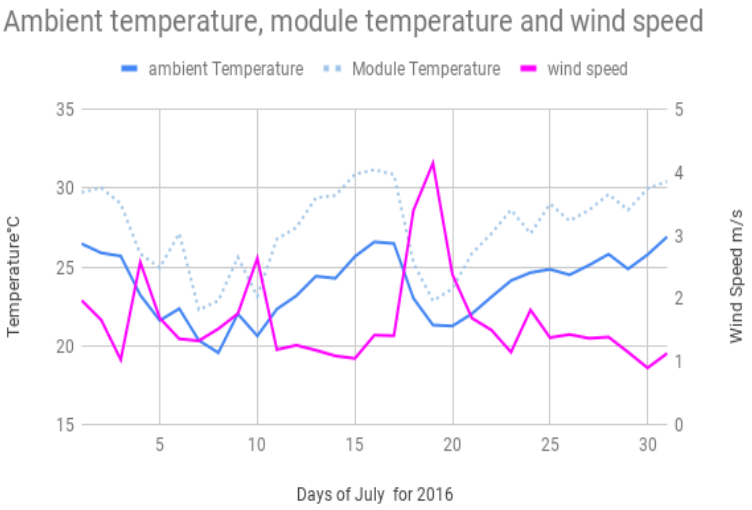

Data Source: Alteso

Figure 37: Temperature plotted against wind speed July 2016.

Ambient temperature (shown above in Figure 37) is mirrored by module temperature in pattern but higher in actual temperature than ambient, while wind speed shows spikes that show some effect on simultaneously reducing ambient and module temperatures.

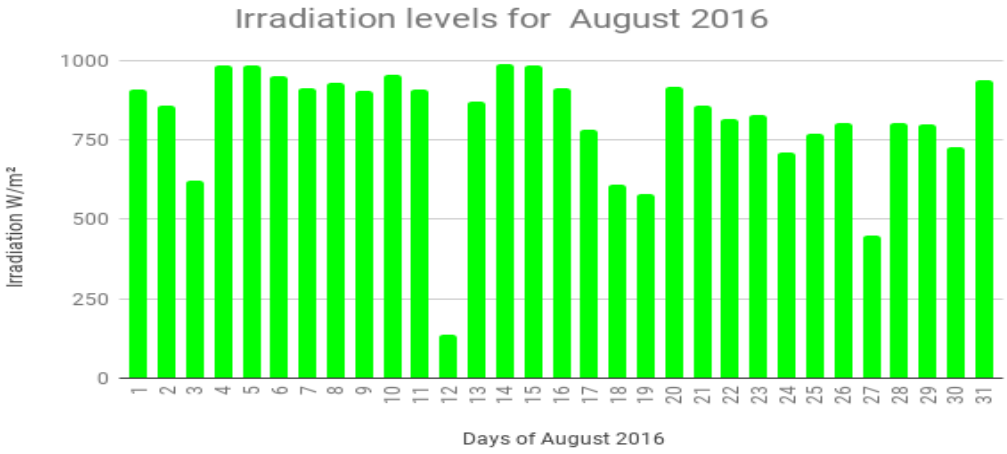

Data Source: Alteso

Figure 38: Irradiation levels August 2016

In comparing Day 6 average irradiation of 952.17 W/m² with a day 10 average of 953.4 W/m² differences of 14.6% losses are calculated, between PID affected string (red) below and that signified as brown, day 6 average losses are 12.03% when (red)PID string is compared to brown reference string and compared red to yellow string 9.3% difference in averages of the two reference strings was only 5.8% and the other reference string labelled yellow was 9.4% in comparing the two reference strings the difference is a mere 5.8% on Day 10.Losses were calculated from differences between good and bad strings and expressed as percentages. Irradiation values can be seen above.

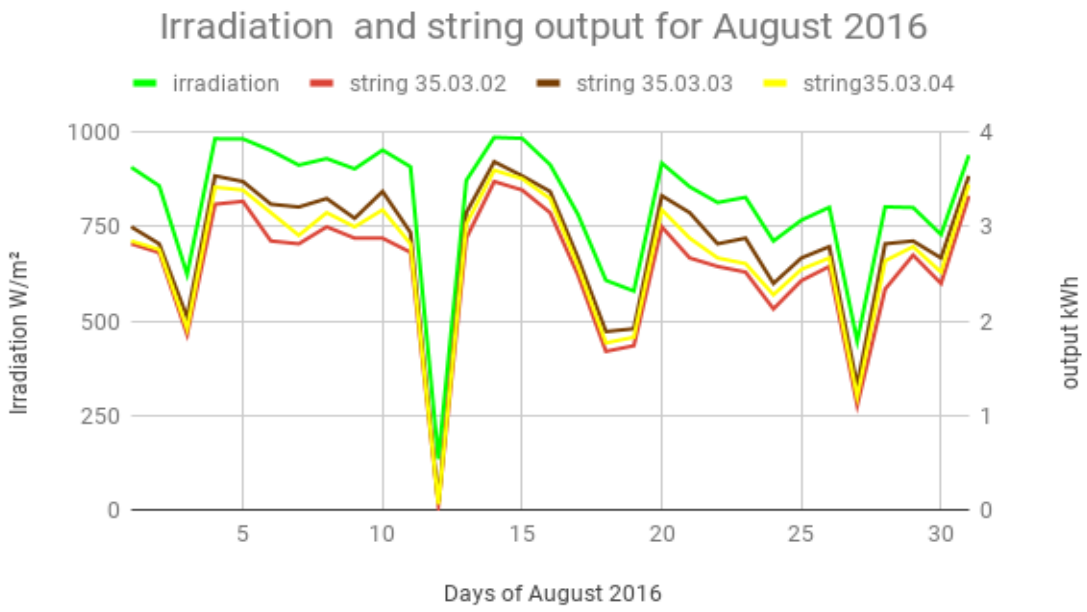

Data Source Alteso

Figure 39: Irradiation against output August 2016

In August of 2016 the trend of output is similar to the pattern created by levels of recorded irradiation and are simultaneously reactionary. The reactions are occuring on the same days but the differences in performance are visible, The differences are observed on day 5 and Day 10 when irradiation levels are similar between these two days great as 12.03% losses are experienced between the PID string (red) and the neighbouring strings represented in brown and yellow (see above figure 39)

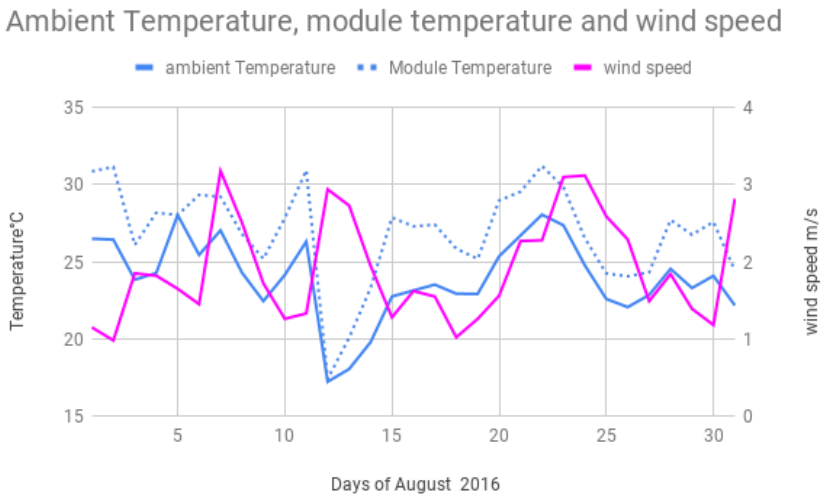

Data Source: Alteso

Figure 40: Temperature against wind speed August 2016

In August it is observed that wind speed is at best between 1 an 3 m/s and its clearest influence could be drawn from days 10 through 14 when wind speeds are above 2m/s and ambient and module temperatures fall to below 18 °C. (See above fig 40)

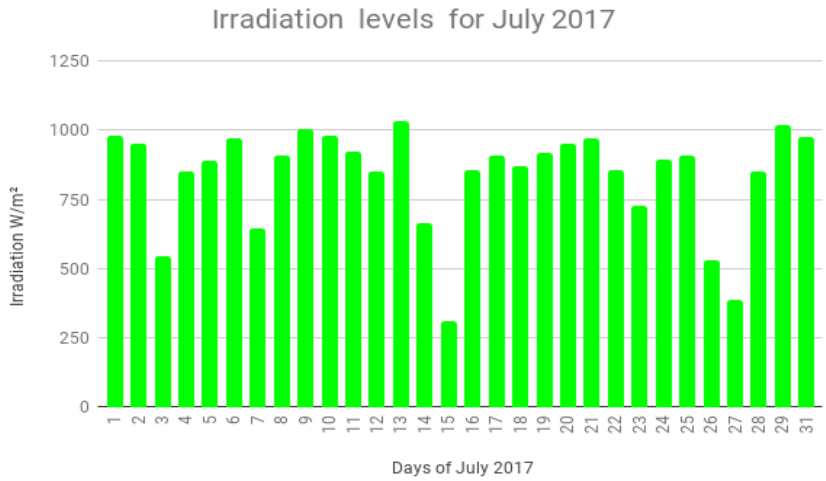

Data Source: Alteso

Figure 41: Irradiation levels for July 2017

Days with average daily irradiation values are selected for comparison for not longer in duration than 12 days. In instance one, day 1 with irradiation levels measured at 981.21 W/m² against that of day7 with average radiation values of 970.02 W/m². PID string (red) compared to reference string brown has average losses of 4.5%, while PID string (red) compared to string labelled yellow had losses of 4.3%. If reference strings are compared to each other brown vs. yellow losses are on average 4.2%.

Day 7 Comparison of Irradiation levels of 970.02 W/m², PID string (red) against, reference string brown losses of 6.7% is experienced, PID string red compared to string yellow saw losses of 2.63%, the difference between the two reference strings is again 4.2% The summary table can be seen below.

Case 2: Comparing Day 11 and 22. Irradiation values of 326.9W/m² and 323.84W/m² respectively.

Table 7: Comparative radiation levels with comparison of losses

July 2017	Irradiation value W/m²	Red vs. Brown %	Red vs. yellow %	Brown vs. yellow %
Day 11	980.73	5.6% diff	3.3%	2.4%
Day 22	971.52	7.0%	2.6%	4.4%

Data Source: Alteso

From the table above it recognised that average percentage losses on the day is greater on the reference string red(PID) vs. the brown ,that of the yellow and red string comparisons, however losses on brown and yellow string comparisons are not always less than that of the PID affected string as evidenced on day 22.

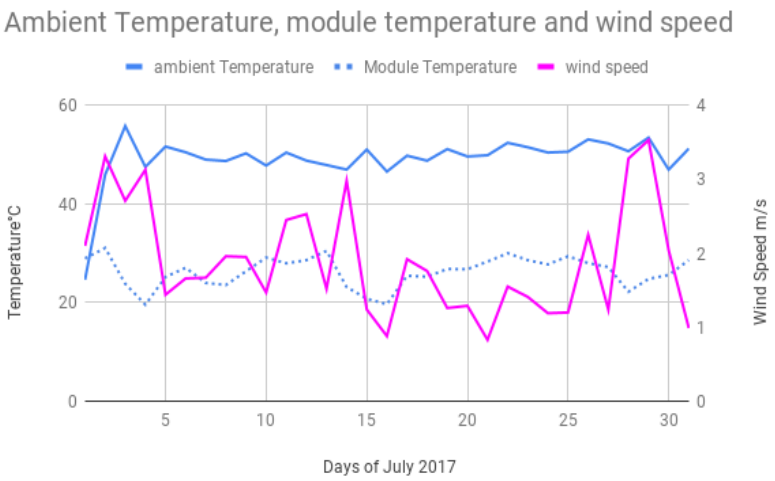

Data Source: Alteso

Figure 42: Temperature plotted against wind speed for July 2017

The figure above shows temperatures against wind speed, the peculiarity of ambient temperature being substantially higher than module temperature in July is alarming and wind speeds above 3m/s have no visible effects on reducing temperature of ambient air. But a slight effect can be seen only on module temperature. Days 3-5 are the only seemingly normal days for the relationship between wind speed and ambient temperature correlation.

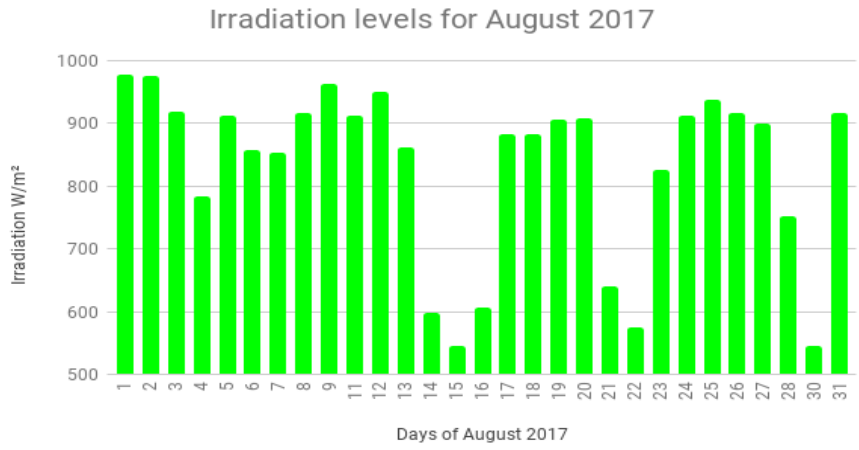

Data Source: Alteso

Figure 43: Irradiation levels for August 2017

Comparisons of Irradiation levels for days with similar irradiation averages and their percentage losses are shown below in table 8 and irradiation levels visible above.

Table 8: Irradiation levels and comparative losses for August 2017

August 2017	Irradiation values W/m²	Red vs. Brown %	Red vs. yellow	Brown vs. yellow
Day 11	911.4	13.5% diff	8.07%	6.1%
Day 24	912.6	6.1%	2.71%	3.5%

Data source: Alteso

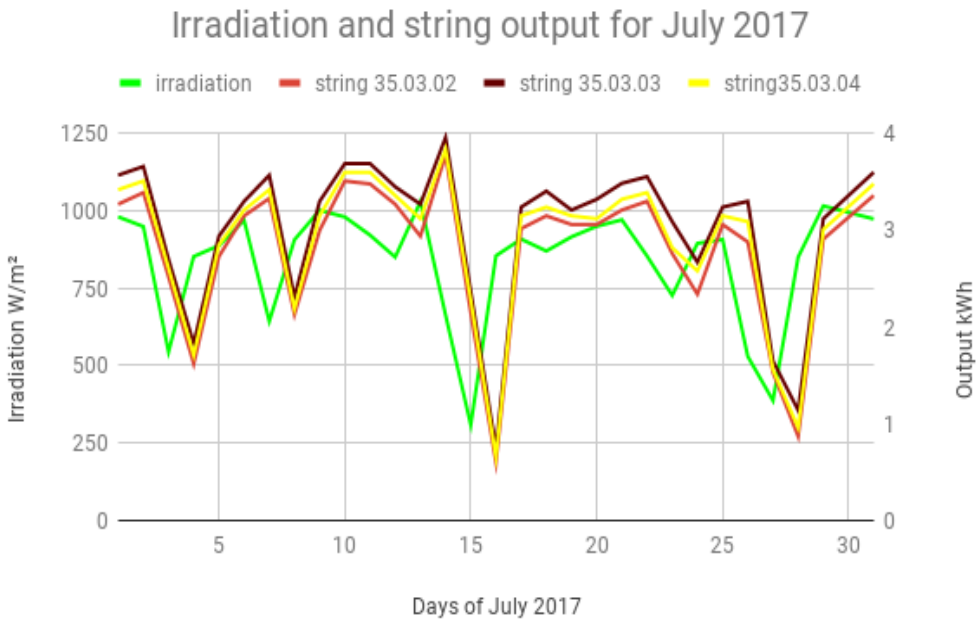

Data Source: Alteso

Figure 44: Irradiation and string output levels for August 2017

Output is following the trends set by irradaition levels but as is now normal (PID) red is visibily underperforming its neighbours. Reference string brown out performs the others as shown above in figure 44.

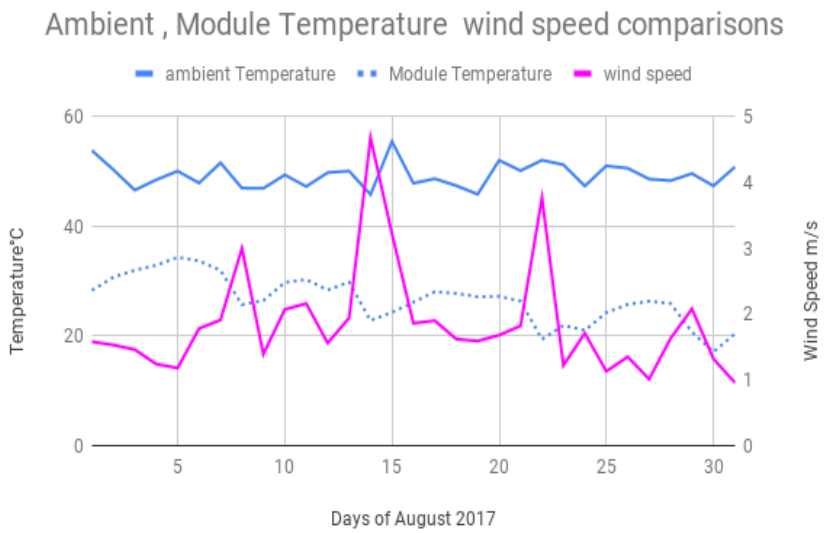

Data Source: Alternative Energy Solutions

Figure 45: Temperature against wind speed for August 2017

Wind Speed is high in general but ambient temperature is seemingly un-reactive to spikes in wind speed. This can be seen in Figure 45 above.

Table 9: Shows specific daily production losses with Irradiation above 305 W/m² after remediation for the study Period over three years.

Dates	Day number	35.03.02 (kWh)	35.03.03 (kWh)	35.03.04 (kWh)	Calculated losses %
2015July	20	1044	1083	1086	3.8%
	25	1020	1062	1065	4.4%
		26,070	27,537	27,288	4.4%
2015 August	4	903	960	936	5.9%
	11	891	945	933	5.7%
		22,734	24,438	23,964	6.9%
2016 July	2	1008	930	1002	7.7%
	6	927	972	951	4.6%
		26,193	28,104	27,291	6.7%
2016 August	6	825	939	909	12.1%
	20	837	972	918	13.8%
		22,137	24,324	23,208	8.9%
2017 July	7	960	1035	990	7.2%
	11	1008	1068	1,044	5.6%
		23,181	25,161	24,140	7.8%
2017 August	11	840	966	906	13.0%
	24	930	990	957	6.0%
		23,550	26,151	24,552	10.5%

Data source: Alteso

From table nine above specific production losses can be seen at varying comparable days with similar levels of radiation across 2015, 2016, 2017 all showing losses across the same periods across the three years as well as from a monthly perspective and progression of losses for across the three years.

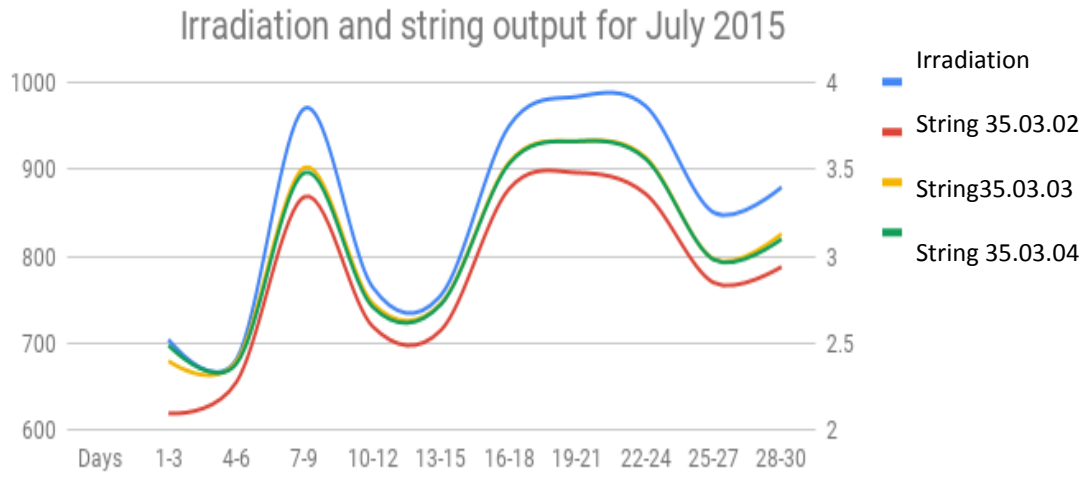

Data Source: Alteso.

Figure 46: Three day string output and average Irradiation for July 2015.

3 day averages are more concise and a better representation of the occurrences and the correlations between measured irradiation, and the output of the strings from the PV plant. On closer inspection its clear all three strings fluctuate with irradiation across the three days, string 35.03.02 (red) which is a affected by PID produced 10% less power than its neighbouring strings 35.03.03(good) and 35.03.04strings. As evidenced above in figure 46.

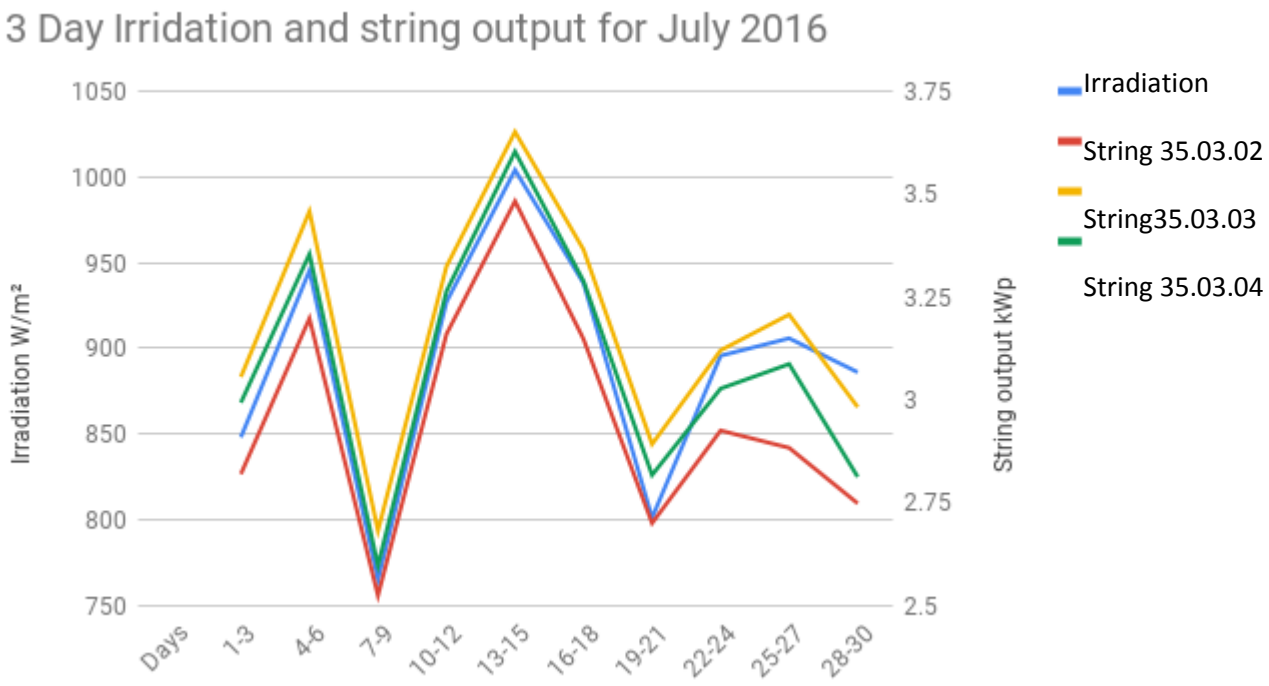

Data Source: Alternative Energy Solutions

Figure 47: Three day average string output and irradiation for July 2016

The problem is not readily visible on this chart of power output in July 2016, the strings are all reacting to the irradiation in real time, the strings 35.03.03(good) and that of string 35.03.04 are close in performance, while string 35.03.02 (red) performs at a lower level than the neighbouring strings. The relative under performance of string 35.03.02(red) is clearly visible in figure 47 above.

Table 10: Shows three day averages and losses for July 2016.

Days	Irradiation W/m	Ambient temp. (°C)	wind speed (m/s)	String 35.03.02 (kWh)	String 35.03.03 (KWh)	string 35.03.04 (kWh)	% losses
1-3	848.1	26.03	1.55	2.81943	3.0555	2.99304	7.7%
4-6	945.303	22.401	1.877	3.1974	3.4578	3.3537	7.5%
7-9	765.099	20.652	1.541	2.5242	2.682	2.5971	6.3%
10-12	927.057	22.049	1.701	3.1596	3.324	3.2637	4.9%
13-15	1003.974	24.42	1.186	3.4824	3.651	3.603	4.6%
16-18	937.89	25.42	2.116	3.147	3.3645	3.288	7.2%
19-21	801.165	21.542	2.741	2.7	2.892	2.817	6.6%
22-24	895.65	23.97	1.49	2.925	3.12	3.027	6.2%
25-27	905.814	24.83	1.398	2.883	3.207	3.0867	10.1%
28-30	886.02	25.4	1.15	2.748	2.982	2.8125	7.8%

Data Source: Alteso

In table 10 above actual 3 day output figures are presented for July 2016, spanning almost the entire month figures of an affected PID string(35.03.02) along with its two unaffected neighbours (35.03.03 ,35.03.04) the general output is clearly distinguishable from that of the reference strings and by all other preceding figures.

The losses during three day averages range from 4.6% to 10.1% as evidenced above. The losses accrued have no specific pattern even on days with similar conditions; they are seemingly unpredictable with the method used.

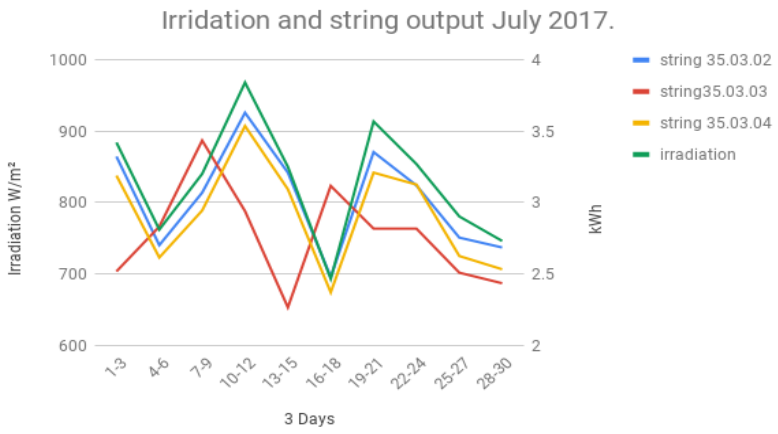

Data Source: Alteso

Figure 48: Three day average string output and irradiation for July 2017

Immediately recognisable from the figure 48 is the fact that that the red line 35.03.02 (red) is not operating like the others, it peaks earlier and at a lower level than the neighbouring strings, the dips are also experienced earlier than the neighbouring string. String 35.03.02 (red) is underperforming its nearest neighbours clearly, day 16-18 the strings are operating where the red is at a high whilst the others are at their lowest.

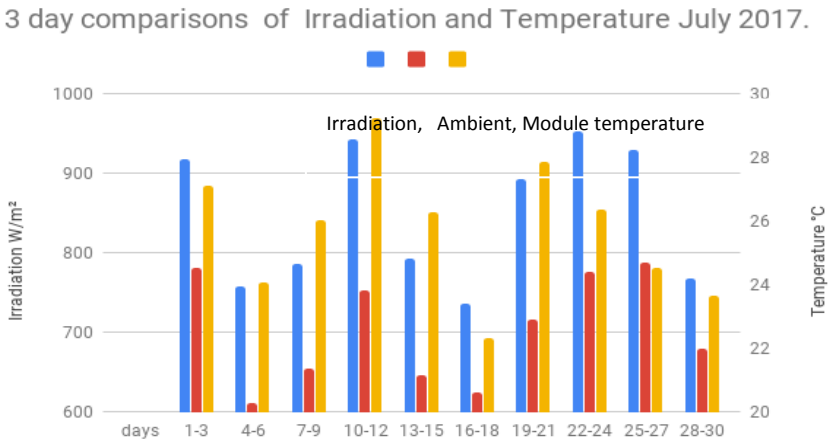

Data Source: Alteso

Figure 49: Three day comparison of Temperature and Irradiation for July 2017

Three day averages are more accurate glimpses into the strings activities and their environmental interplay. The three day irradiation averages show greater fluctuations in

irradiation, the influence is likely due to humidity and rainfall and to a lesser extent from the wind. Day 1-3 and 25-27 show the highest levels recorded for the month as seen above in figure 49 above.

Table 11: Shows three day averages and losses for July 2017.

Days	Irradiation W/m²	Ambient temp. (°C)	wind speed (m/s)	string 35.03.02 kWh	String 35.03.03 kWh	string 35.03.04 kWh	% losses
1-3	884.241	24.51	20.71	3.3228	3.3228	3.189	24.2%
4-6	762.03	20.26	2.077	2.7012	2.7012	2.6145	4.2%
7-9	840.2499	21.34	1.86	3.0693	3.0693	2.9442	19%
10-12	968.37	23.81	2.15	3.63	3.63	3.537	19%
13-15	850.1007	21.16	1.914	3.21	3.21	3.093	29.4%
16-18	693.063	20.60	1.52	2.478	2.478	2.37	20.5%
19-21	913.71	22.90	1.13	3.354	3.354	3.21	16.0%
22-24	853.98	24.40	1.38	3.12	3.12	3.126	9.7%
25-27	780.51	24.69	1.56	2.754	2.754	2.625	8.9%
28-30	746.1	21.97	2.96	2.685	2.685	2.532	9.3%

Data Source: Alteso

From table 11 above, in general for 2017, the evidence suggests that underperformance is still visible, yet three day averages could mislead as seen on day 7-9, 16-18, where average production is seemingly higher on the affected string. Overall red string performance is generally lower. Losses vary from a high of 29.4% to 8.9% as evidenced above. Mid month average losses were the worst at 29.4%. A bit of a stretch from the performance gains expected with the addition of a PIDbox. Losses are calculated by taking the difference

between the best performing string from above and the worst performance string and expressed as a percentage.

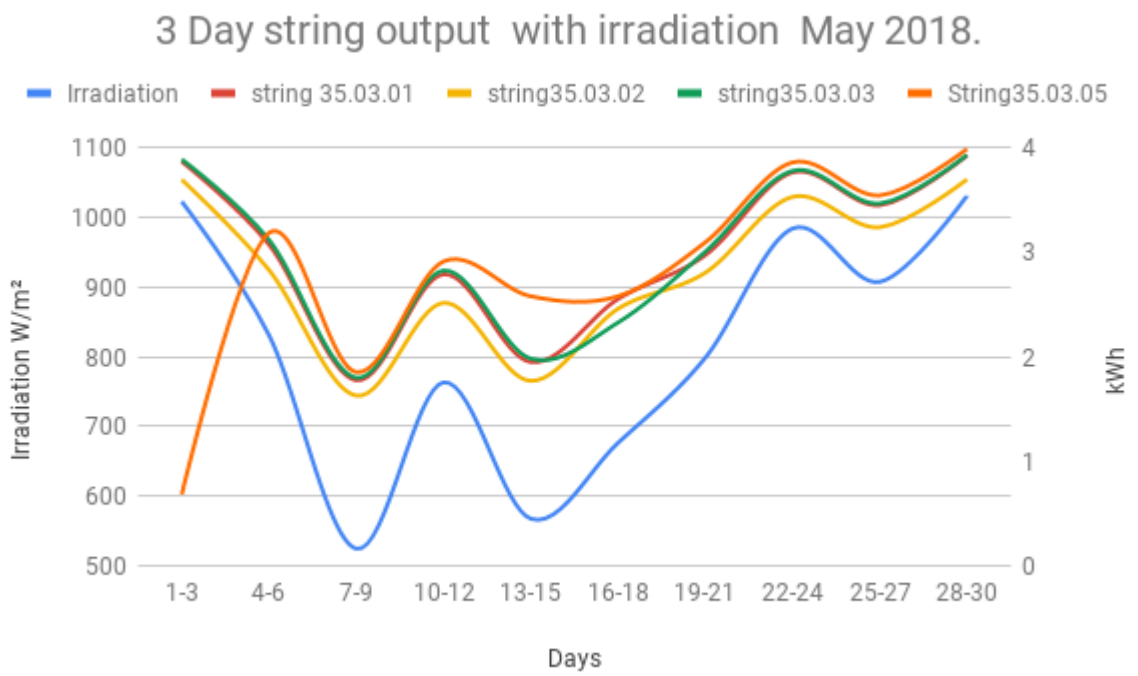

Data Source: Alteso

Figure 50: Three day string output averages for May 2018

In comparing irradiation to output see figure 50 above, a direct relation between irradiation and output is visible, the output is responding to incoming irradiation, the strings are performing similarly and in a close range, their behaviour is visually similar and at times intersecting. Converting and producing only as much as the neighbouring strings. The string 35.03.02 red continues underperforming its neighbours in general for the month but an improvement on it performance from the previous year is noted. From the four strings selected it would appear the best performing string it 35.03.05 (green), indicative of the fact the string is uninfected by PID, The strings neighbouring on the left and right of 35.03.03 are almost identical in behaviour.

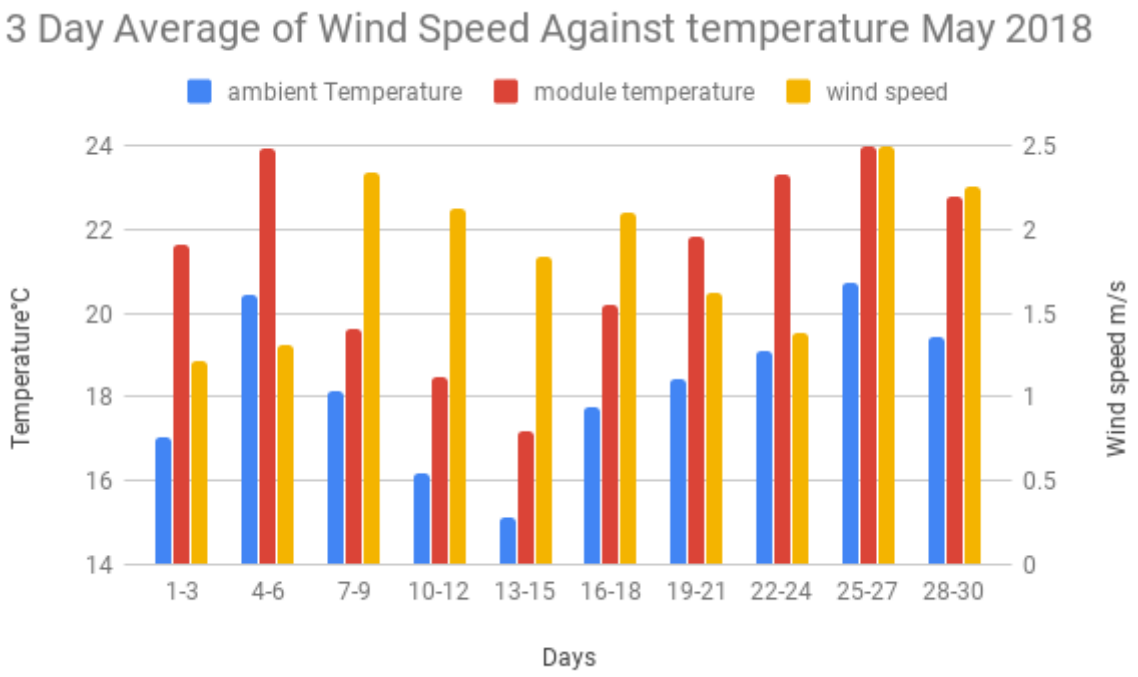

Data Source: Alteso

Figure 51: Three day average wind speed plotted against temperature for May 2018

For the same period over the course of May 2018 see figure 51 above, The expectancy of module temperature being higher than ambient temperature is present and at times as 4°C a higher than ambient temperature and when wind speeds are above 1.5 m/s module temperatures were relatively low between the 10th and the 12th of May and much higher between the 25th to the 27th and again between 28th and 30th of May.

Table 12: Three day averages and corresponding losses for May 2018

Days	Irradiation W/m²	Ambient Temp (°C)	Wind speed (m/s)	string 35.03.01 kWh	String 35.03.02 kWh	String 35.03.03 kWh	String 35.03.05 KWh	% losses Best-worst string
1-3	1022.985	17.01	1.22	3.87	3.696	3.891	0.6831	82.4%
4-6	831.183	20.44	1.315	3.075	2.832	3.12	3.1875	3.4%
7-9	524.604	18.162	2.34	1.776	1.629	1.8	1.854	12.1%
10-12	763.41	16.2	2.13	2.79	2.517	2.826	2.91324	13.6%
13-15	567.57	15.14	1.84	1.95	1.77	1.9824	2.58	24.4%
16-18	676.395	17.74	2.1	2.553	2.46	2.328	2.58	9.7%
19-21	798.618	18.43	1.62	2.973	2.805	3.006	3.096	9.3%
22-24	984.18	19.12	1.381	3.765	3.531	3.78	3.861	8.5%
25-27	907.668	20.74	2.494	3.4512	3.24	3.468	3.5451	8.6%
28-30	1031.298	19.46	2.252	3.927	3.699	3.933	3.99	7.2%

Data Source: Alteso

Table12: Above demonstrates actual figures tabulated from the three day averages for the month of May 2018.

The general illustration shows no recovery from PID, continued losses on the PID affected string as shown in its underperformance above. The losses can be seen in the column on the right; the varying losses from day 1 to day 30 are as high as 82.4% Losses are the percentage difference between the best producing reference string and the worst string affected by PID in most cases the red string 35.03.02. The variation is most peculiar from day 4 to six when the losses are reduced to a mere 3.4%.

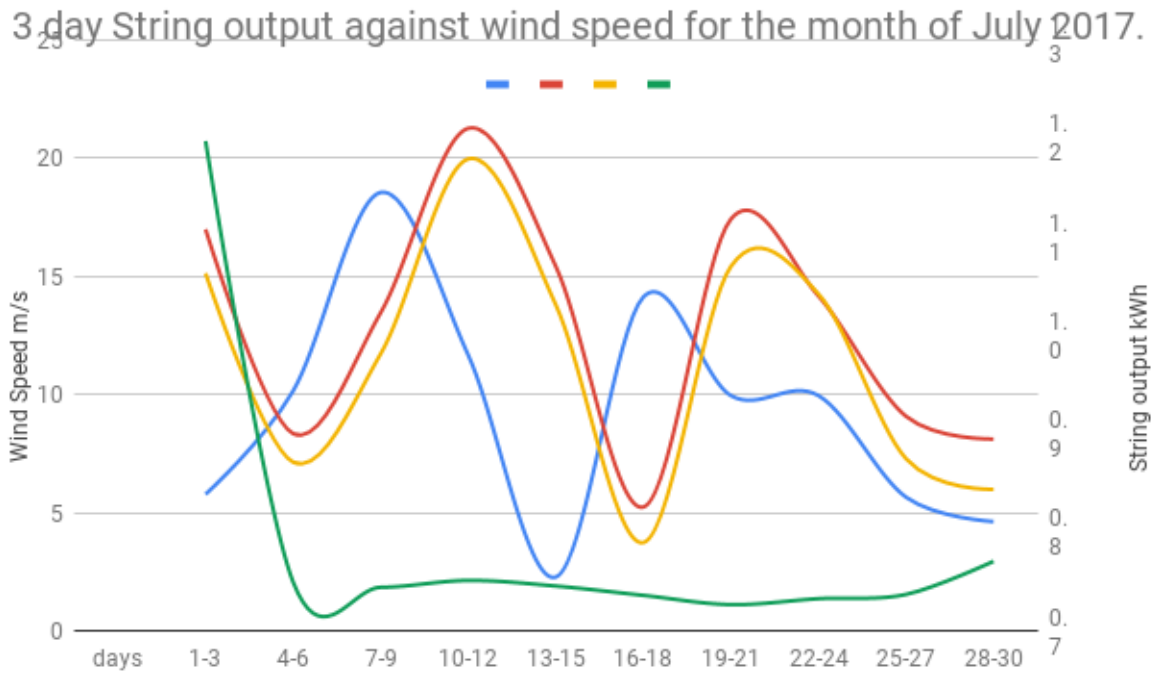

Data Source: Alteso

Figure 52: Three day string average output for May 2018

The strings are performing differently during the monthly of July 2017 (see Figure 52 above), the string represented in blue which is identified as 35.03.02 is one identified by initial testing as infected with PID. The a probable explanation of the losses would be affected strings will operate at lower voltages than those unaffected by PID .The modules in the strings are required to deliver the same power as the other strings on site,(losses are 10% less than its neighbouring strings) The curves of the red and yellow strings behave synchronously, while the green line represents wind speeds at 3 day averages, the wind averages appear to be almost monotonous despite the fluctuations in string performance, it is fair to note wind speed in this regard does little to affect the string output within the PV park.

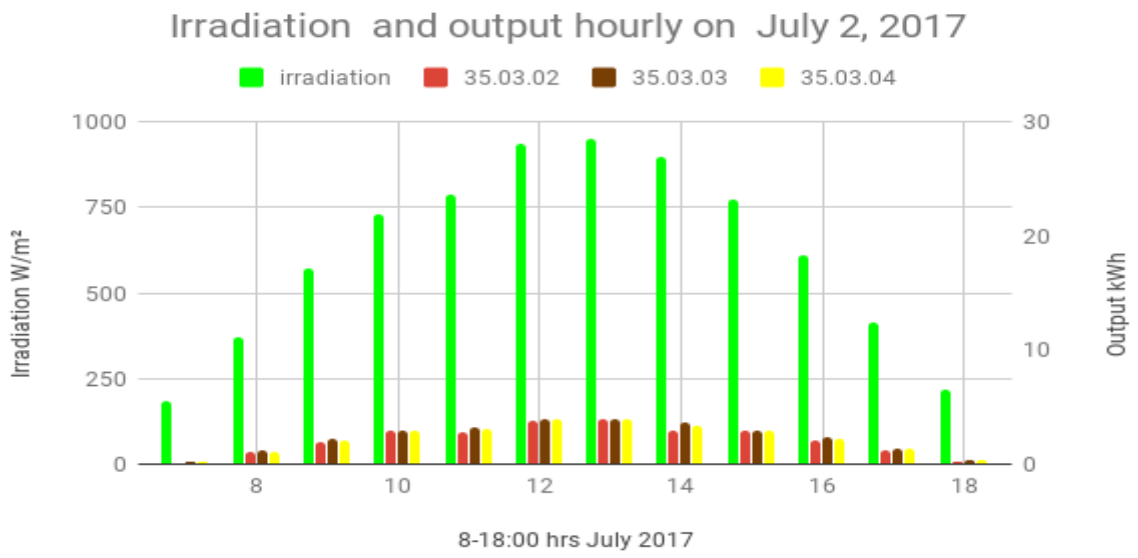

Data Source: Alteso

Figure 53: Irradiation against output progression for July 2, 2017.

The solar progression is shown over the course of a day for the second of July, 2017. Between peak period 12:00 hrs and 14:00 hrs appears to be the best time for harvesting the energy of the sun see figure 53 above.

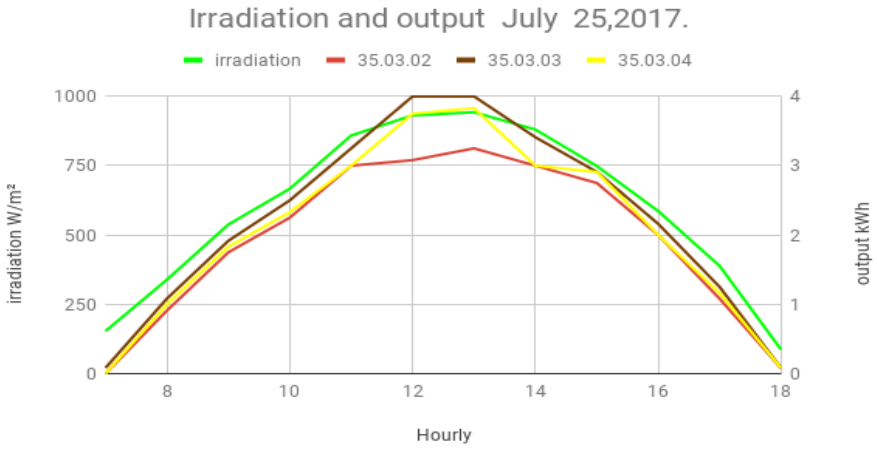

Data Source: Alteso

Figure 54: Specific irradiation and output values for 25th July 2017.

Specific irradiation and output values have been plotted (see figure 54) to reflect progression over the course of a day, this being the 25th of July, 2017 for comparison to figure 53 above.

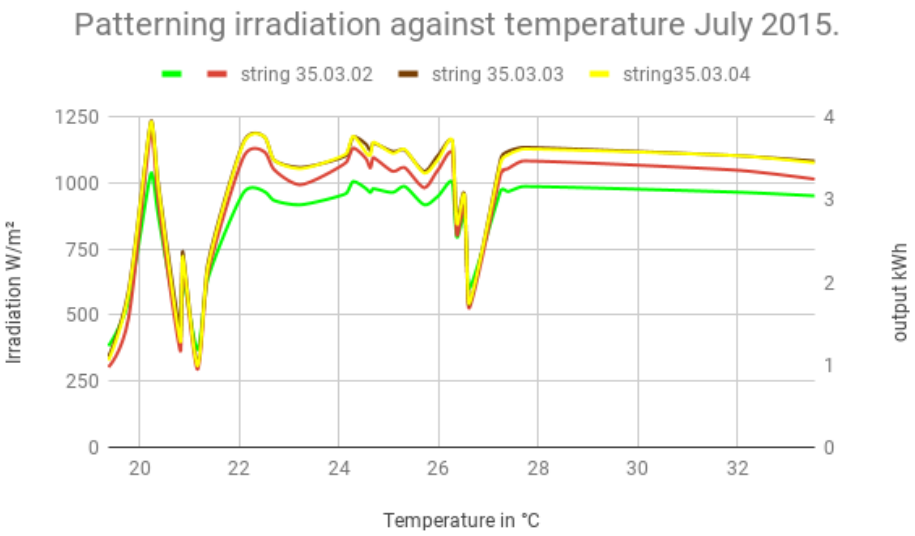

Data Source: Alteso

Figure 55: Patterning Irradiation and output against temperature July 2015.

Figure 55 shows irradiation levels at different temperature values at 21°C and 27 °C it is observed that irradiation is measured at lower levels than at 20° C and upwards

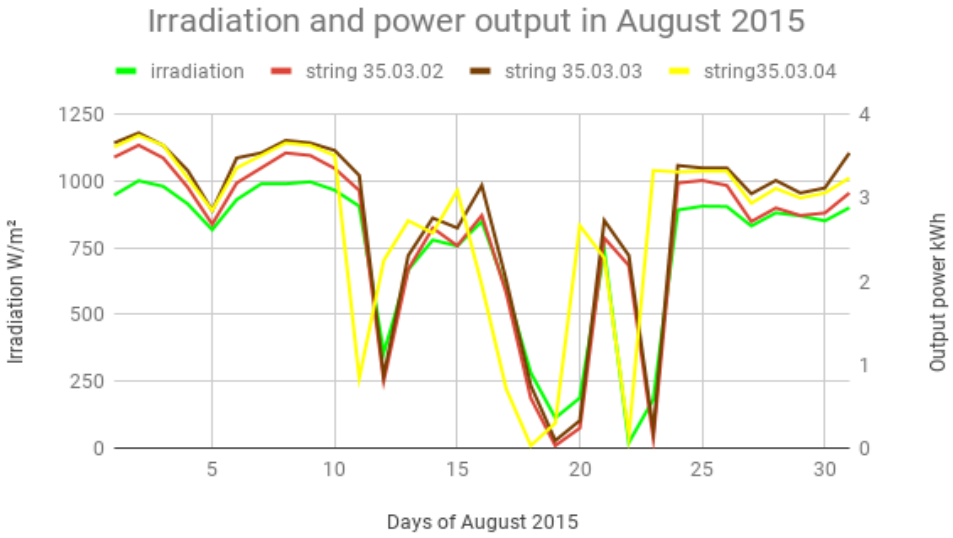

Data Source: Alteso

Figure 56: Patterning Irradiation and output against temperature August 2015

Similar to above in Figure 56 irradiation was again plotted at different temperature values and the result was much different from figure 55, which is much more erratic than in figure above.

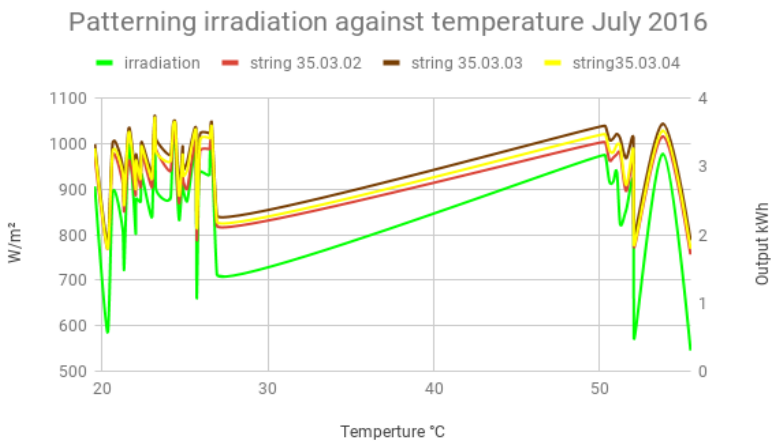

Data Source: Alteso

Figure 57: Patterning Irradiation and output against temperature July 2016

Similar to above irradiation was plotted against various temperatures, erratic and different from the previous two comparisons in figures 55 and 56, between 29° and 50° a slight increase is illustrated in irradiation before and after that seismic fluctuations are seen.

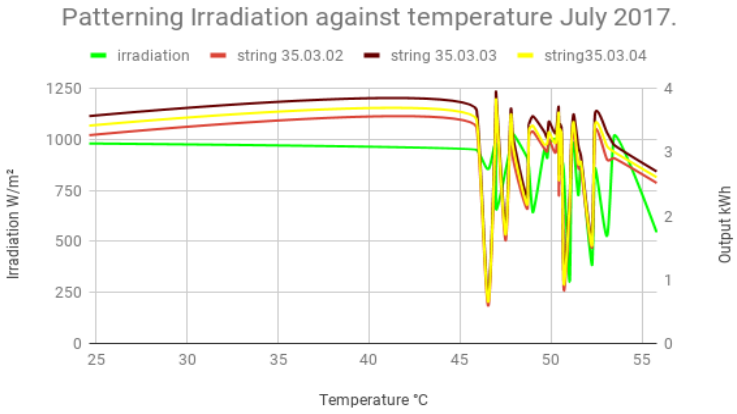

Data Source: Alteso

Figure 58: Patterning Irradiation and output against temperature July 2017

From patterning in figure 58, between 27°C-32°C during July of 2017 after the diagnosis of PID its is observed that 3.5 kWh per string in output is produced from measured irradiation of

999 W/m², an erratic pattern is seen in performance extending to 45.9°C with similar output being observed of 3.7kWh on the unaffected strings in comparison.

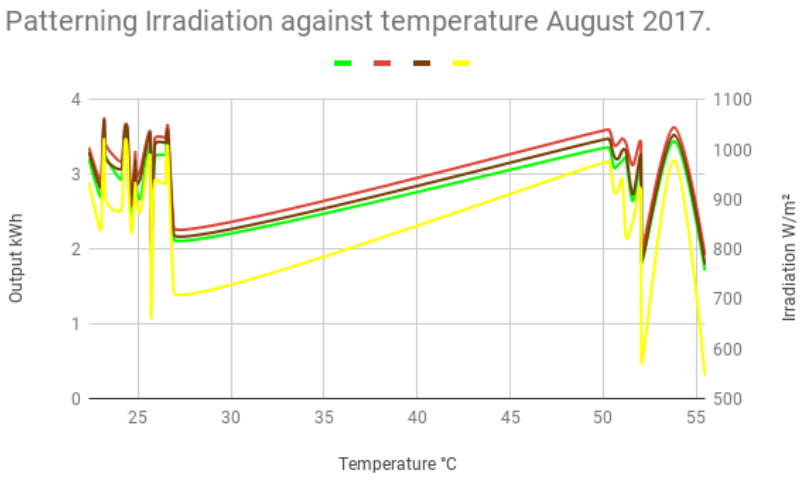

Data Source: Alteso

Figure 59: Patterning Irradiation and output against temperature August 2017

In August of 2017 from figure 59 above, temperatures were on average higher than the previous years and no constants in production are readily identifiable. Patterning previously examined temperature ranges a, show no concomitant relation between temperature and irradiation. No particular repetitive pattern can be identified.

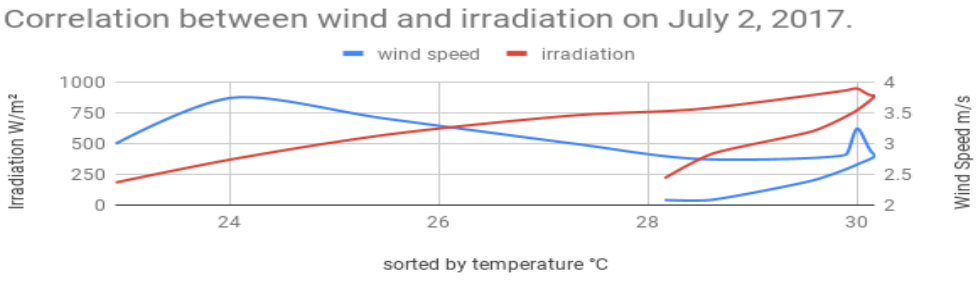

Data Source: Alteso

Figure 60: Correlating wind to Irradiation July 2, 2017.

In the figure 60 above the interplay between temperature Irradiation and wind speed show decreases in wind speed a concomitant increase in irradiation levels are observed and at 27°C irradiation is recorded at 732 W/m² , specific output at this measurement is 3kWh on the reference strings and 2.91kWh on the (red) PID string, this occured at 10 a.m.

Table13: Daily progression of parameters presented on day of similar average irradiation as below and percentage losses.

July2	Irradiation W/m²	ambient temperature °C	module Temperature °C	wind speed m/s	35.03.02 kWh	35.03.03 kWh	35.03.04 kWh	% losses
7	182.83	22.91	24.08	3	0.083	0.16	0.16	48.1%
8	369.66	24	27.83	3.75	1.08	1.25	1.08	13.6%
9	574.16	25.5	32.75	3.41	2	2.25	2.08	11.1%
10	732.75	27.3	37.25	3	2.91	3	3	3%
11	786.08	28.5	40.25	2.75	2.75	3.16	3.08	10.7%
12	937.83	29.9	45.5	2.83	3.83	4	4	4.3%
13	953.16	30	45.5	3.25	4	4	4	0
14	897	30.16	45.3	2.83	3	3.6	3.3	16.6%
15	775	30	43.4	2.66	3	3	3	0
16	609.75	29.6	40.6	2.41	2.08	2.3	2.16	9.5%
17	414.25	28.6	36.16	2.08	1.25	1.41	1.33	11.3%
18	218.16	28.16	31	2.08	0.25	0.41	0.33	39%

Data Source: Alteso

Specific production on this day between the specified intervals is 298kWh on the affected (35.03.02), 317 and 308kWh on the reference strings. The losses accrued are calculated at 5.9% on the day by expressing the accumulated difference between the PID string and the good strings.

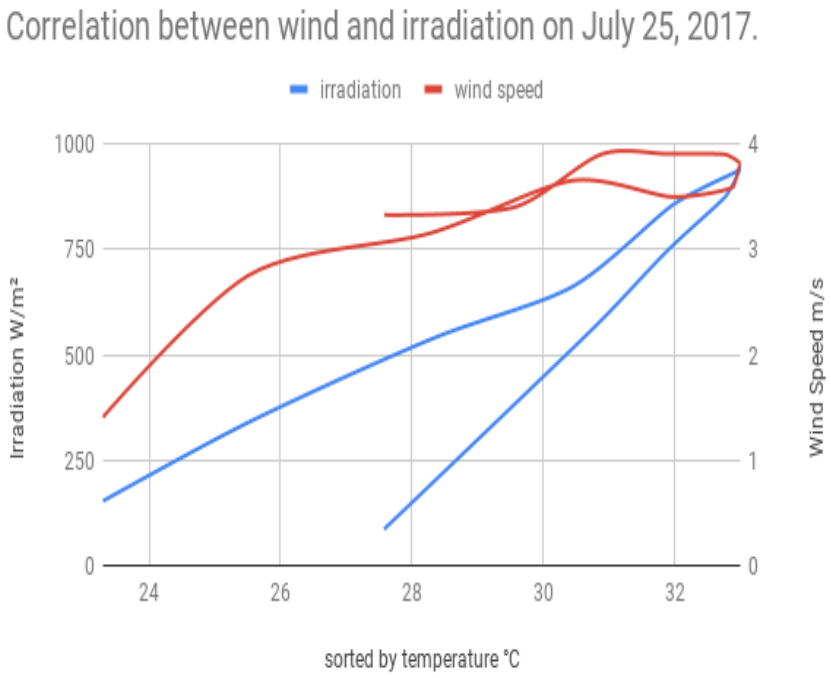

Data Source: Alteso

Figure 61: Correlating between wind and irradiation July 25, 2017.

From this Figure 61 the relationship is different to that recorded on the second of July, as temperature increases so does wind speed and recorded irradiation levels.

Table14: Daily progression of parameters presented for 25th July 2017.

July25	Irradiation W/m²	ambient temperature °C	module Temperature °C	wind speed m/s	35.03.02 kWh	35.03.03 kWh	35.03.04 kWh	% losses
7	153	23.3	23.08	1.41	0	0.083	0	0
8	339	25.5	28.75	2.75	0.91	1.083	1	15.9%
9	537	28.3	35.3	3.16	1.75	1.916	1.83	8.60%
10	666	30.5	39.5	3.66	2.25	2.5	2.33	10%
11	858	32	42.8	3.5	3	3.25	3	7.60%
12	931	32.9	45.08	3.6	3.08	4	3.75	10%
13	942	33	45.08	3.8	3.25	4	3.83	18.70%
14	880	32.8	43.5	3.9	3	3.41	3	12%
15	748	31.9	40.83	3.91	2.75	2.91	2.91	5.40%
16	586	30.91	38.16	3.91	2	2.16	2	7.40%
17	388.16	29.6	34.6	3.41	1.08	1.25	1.16	13.6%
18	86.5	27.58	28.6	3.33	0.08	0.08	0.08	0

Data Source: Alteso

Both days have on average similar comparable levels of irradiation and are the wind effect on the temperature is seemingly non-existent. Temperature climbs as irradiation soars (see table 15 above), the losses calculated above are a subtraction of the value of the best production value from the unaffected string subtracted from the value of the worst producing PID string and expressing this loss as a percentage. Specific production on this day was specified is 310kWh on the affected, 334 and 328kWh on the reference strings. The losses accrued are calculated at 7.1% on the day. Over the 23 day span, where irradiation levels are similar and experienced at similar times of the day, an increase of 4% in losses is experienced.Specific production on these two days with similar irradiation values at similar times in comparison are shown below.

Table 15: Progression of losses throughout two solar days at peak production July 2, 25

Date	Time	Irradiation W/m²	Ambient Temp. °C	Wind speed m/s	35.03.02 kWh	35.03.03 kWh	35.03.04 kWh	Specific losses
July 2	12 p.m.	937.83	29.9	2.83	3.83	4	4	4.2%
July 25		931.66	32.9	3.6	3.08	4	3.75	10%
July 2	13hr	953.16	30	3.25	4	4	4	
July 25		942.75	33	3.8	3.25	4	3.83	18.7%
July 2	14hr	897	30.1	2.83	3	3.6	3.3	16.6%
July 25		880.33	32.8	3.9	3	3.41	3	12.0%
July 2	15hr	775	30	2.66	3	3	3	
July 25		748.5	31.9	3.91	2.75	2.91	2.91	5.4%
July 2	16hr	609.75	29.9	2.41	2.08	2.3	2.06	9.5%
July 25		586.08	30.91	3.91	2	2.16	2	7.4%
July 2	17hr	414.25	28.6	2.08	1.25	1.41	1.33	11.3%
July 25		388.16	29.6	3.41	1.08	1.25	1.16	13.6%
July 2	18hr	218.16	28.16	2.08	0.25	0.41	0.33	39.02%
July		86.5	27.58	3.33	0.08	0.08	0.08	

Data Source: Alteso

The above table16 shows the specific production losses for two days July 2 and the 25 July the comparison is across a 7hr period at the peak irradiation period from midday to 18hr levels were measured at their highest above 900m/s²

Losses are lower at high irradiation on both days 4.2% and 10% at 12p.m.

It increases in the next hour on the 25th to 18.7%, while it's nullified on the 2nd of July at the same time as seen above.

Losses reduce to their lowest level possible on the 2nd July while to 5.4% at 13 hr on the 25th, but again increasing losses of 39.2% at 18hr and again no losses are registered across the same strings on the 25th. Specific production losses between the two days increased from 8% to 12.9% over the same time intervals.

In comparison filtering the data for the previous year on the 25th of July filtered losses amounted to 5.99%, in order to filter the effects of wind and temperature a condition of no wind speed is recorded , and(+/-5°C) the affected string produced 298kWh on the day while on the unaffected,317kWh ,308kWh on the reference strings.'

3.3 Attempted Discovery of method of early detection

In comparison to the 2nd of July as filtered above the affected string had actual production figures for the day of 310 kWh, while the unaffected had 334KWh and 328kWh .The losses calculated on the difference in the two amounted to a loss of 7.18% on the day. In this regard it can be safely assumed that wind's impact is avoided and that of ambient temperature

For 2017 none of the above criteria could be met for the two specified days as such no true pattern could be identified from filtering. No unusual pattern or could a clearer pattern be discerned. Using this method illustrates a linear movement, rather than a curve after filtering, increasing temperature and wind speed is experienced throughout the morning to early afternoon and sudden drops at approximately 16 hr with further fluctuations into sunset hours at 18hr.From the methods used in this Master's thesis, it was not possible to develop an early detection system through patterning of the filtered data.

4. Summary and Conclusion

In this section a summary and a conclusion will be presented of the major factors recognised in this study and their interplay.

From an annual perspective, it is extremely difficult to identify the changes in module temperature using long or short data intervals which effectively affects the accuracy of the results, the picture given is not very specific. The averages produced give vague snapshots in actual performance; the appearances are deceiving and would not accurately represent aggravating effects of PID adequately, unless the changes were having a more sustained effect during a year or during months outside of the study window. If the changes were more than 10% over the course of 4 days (15 hr solar days each), then the changes would possibly be more visible in the data when averaged. It is a certainty that averages for the indicative parameters, such as irradiation experienced over a three day period would be more favourable than that of a whole month, in the identification the effects of PID. A figure of the year 2016 shows the average irradiation for the entire month of July was 887.7W/m², in comparison to the three day average between the hours of 10a.m.-12p.m. alone, the average was 968.1 W/m². It is important to note that the usage of annual averages to identify PID is not recommended for the simple reason that it lacks detail that would otherwise falsely indicate PID. The study conducted was able to clearly confirm recurring and increasing production losses. The losses as a result of PID are demonstrated in tables 9-14.

From the approach of sifting the data from an annual level to identify specific changes, proved rather difficult and further less accurate than from a monthly perspective. Knowing the location of the infection and not how widespread the infection is poses a problem for the operators. The parameters temperature, wind, irradiation, in the quantification process was not adequately representative from an annual perspective. Losses were nevertheless quantifiable and directly attributable PID.

From the figures produced, no real gains have been realised by adding PID boxes to the strings to rectify the problem as evidenced in table 9. Losses have been increasing with time. The underlying issue of growing losses still exist as a result of PID influences.

Production from a monthly level are expectedly high with historically hotter days and higher levels of irradiation influencing higher ambient temperatures and module temperatures, that must also be taken into consideration. The environmental factors do have an effect on the performance of the modules but at the wind speeds recorded, the changes are not always recognisable in reducing temperatures. However, in general high irradiation and increasing wind speed seems to have an effect on lowering temperatures .The expectation of wind having an effect on module temperature can be seen in the many figures produced.

From a three day average perspective the temperature cycles show more accurately that the strings experience (30 day period) irradiation levels that are representative of the fluctuations experienced at large PV plants in their day to day activities. Accuracy of data is paramount, but the probability of finding the affected strings becomes greater with more refined data. Sorting through the data set can be quite overwhelming with standard spread sheet software and without the use of complicated algorithms. Producing the level of data accuracy required from a large dataset is time consuming. Pinpointing the exact days when PID exists would be most difficult when using this method to aid in the confirmation process. Three days of good weather may be more suitable for long term comparisons.

In 2015 losses on an affected string 35.03.02 were calculated to be on average 5.8%.

In 2016 losses on the affected string were calculated to be on average at 6.6%,

In 2017 losses were calculated to be on average 7.06 %

More detailed losses have been quantified on a Daily, Monthly, and Annual basis as seen in the tables 9-13.

In May of 2018 losses on average were calculated at 6.58% considering this as not being near peak harvesting season it would appear losses have been increasing and further remedies should be sought for this PID problem, whether the changing modules in a string, adding more PID boxes, PV guards, or another applicable technology to control voltage and reverse the flow of electrons to their intended flow path to the P- N junctions, another solution should be sought.

In a PV field with 5152 strings in Part two of the site, using this method of to confirm loss on 20 to 30 infected strings from monitoring data without the use of specialised software proves

a daunting task, doing a desk study may be the cheapest method of tracking PID but, not the most effective, it is time consuming and intensive, the environmental factors being used as indicators may present the case of accelerating the impact of PID, the resilience of the modules are ultimately the deciding factor in the energy conversion process, if these don't function as they should then the expected nominal power will not be realised. Close to 90% conversion rates will not be realised, and losses are experienced at all PV plants, the task remains for the operators in controlling or reducing the losses.

During the process of conversion a lot of energy is being lost as heat and the main reason why module temperatures are generally higher than ambient temperature.

The relationship between string and irradiation is clear, from all the figures plotted, the strings react to input from irradiation, the performance of the affected string chosen is constantly below that of the neighbouring strings and losses are seen to increase during the duration of the study as evidenced in table 9-13. Days of similarly high levels of irradiation (peak production days) in the months of July and August, for the years 2015-2017 are displayed. After the repair had been implemented no significant change has been witnessed. The losses could likely be residual, as the repair process does require some reaction time, but the average percentage losses are greater with the effluxion of time which would seemingly indicate that the repair has had little effect up until the end date of the entire dataset.

If a clear pattern is to be seen for future detection, what is known from patterning between 26°C-32°C during July of 2016 and again in 2017 the operating temperature range extended to 45.9°C. An output of 1.1Kwh per string is produced from a measured irradiation of 999 W/m², when the temperature is increased to any higher than 49°C then the performance of all the compared strings become erratic and unpredictable, slightly greater output can be seen for very short bursts during the course of a day. Attempts at finding a method of detection with the resources and methods used in this study through data pattering showed no discernible patterns or irregularities of merit. A better approach to detection would require specialist software which could analyse all the strings with the results obtained from this study and then filter all the unknown factors from daily use to reduce down time in the detection of PID infected strings.

Production levels lower than 1.2 kWh per string with constant levels of irradiation were also observed. In addition this operating range does not hold true for 2016 before the repairs were being implemented for the same period as in 2015 and 2017.

PID boxes seemed to have had little effect on the quantity of losses being experienced at the plant. The https://www.ilumen.be website state that after a few weeks efficiency is expected to be increased on average by 7.5% or minimally by 1.3% and maximally by 16.7% and a few weeks after the installation of a PID box.

4.1 Extrapolation of benefit/loss assumption

If it is assumed a 50% infection rate across the a 10 MW plant site, with the daily loss equalling 7.1% the result of the losses would be the region of 72MWh on the 25th of July alone, again assuming the other 1000 strings are performing optimally and unaffected by any other intrusive factors.

5. Bibliography

Armstrong S. and Hurley W. G., “A thermal model for photovoltaic panels under varying atmospheric conditions,” Appl. Therm. Eng., vol. 30, no. 11–12, pp. 1488–1495, 2010.

Bhattacharya Tanima, Chakraborty Ajoy, Kaushik K, Pal 2014. ‘Effects of Ambient Temperature and Wind Speed on Performance of Monocrystalline Solar Photovoltaic Module in Tripura, India”. Journal of Solar Energy, volume 2014, Article ID 817078, 5 pages retrieved from hindawi.com on June 28, 2018.

D Lausch,V. Naumann, O. Breitenstein,Jan Bauer,Andreas Graff,J.Bagdahn, C, Hagendorf “Potential-Induced Degradation(PID): Introduction of a Novel Test Approach and Explanation of increased Depletion Region Recombination.”, in the IEEE journal of Photovoltaics.Vol.4 NO.3 May 2014, retrieved from https://www-old.mpi-halle.mpg.de/mpi/publi/pdf/11826_14.pdf on 11 August,2018.

Deutsche Gesellschaft für Sonnenenergie Photovoltaische Anlagen (4th edition chapter3 Berlin: Berlin Brandenburg e.V.;2010. from www.Sciencedirect.com retrieved on 20 July 2018.

Hacke P, Smith.R, Prog Photovolt, Res, Appl 22 (2015)775-783 a)
Hacke P, Spataru S, .Teriwilinger.K, Perrin.G, Glick.S, Kurtz. S, Wohlgemuth. J IEEEJ. Photovoltaics 5 (2015) 1549-1553 b)

Jawad R.S, Abass K.I, Alwaeli A , Al –Zubaidi D S M “Dust effect on PV outcomes at five different sites around Baghdad.”The Journal of Scientific Engineering research 49(7):93-102 retrieved from https://www.researchgate.net/publication/319066585_Dust_effect_on_PV_outcomes_at_five_different_sites_around_Baghdad on date September 6, 2018

Kaldellis J. Kapsali K., M., and Kavadias K. A., “Temperature and wind speed impact on the efficiency of PV installations. Experience obtained from outdoor measurements in Greece,” Renew. Energy, vol. 66, pp. 612–624, 2014.

King D.L, Boyson W.E, Kratochvil J.A. 'Analysis of factors influencing the annual energy production of photovoltaic systems from conference record of the twenty-Ninth IEEE Photovoltaic Specialists conference, 2002: p 1356-1361. From www.Sciencedirect.com retrieved on 20 July 2018.

Kurtz S, Whitfield K., Miller D, Joyce J, Wohlgemuth J,, Kempe M, et al. "Evaluation of high-temperature exposure of rack-mounted photovoltaic modules in 34thIEEE Photovoltaic Specialists Conference (PVSC),2009: p.2399-2404. From www.Sciencedirect.com retrieved on 20 July 2018.

Luo Wei, Khoo Yong Sheng,a Hacke Peter, Volker Naumann, Lausch Dominik, Harvey P Steven, Singh Jai Prakash, Chai Jing, Wang Yan, Arm 2016, Potential-induced degradation in photovoltaic modules: a critical review. Energy, Environment and science, Royal society of chemistry. Retrieved from https://www.researchgate.net/publication/310666372_Potential-induced_Degradation_in_Photovoltaic_Modules_A_Critical_Review... on date June 6, 2018.

Martinez-Moreno F, Pigueiras E.L, Munoz J, Moreton R. 2012" On the testing of large PV arrays" Progress in photovoltaics Research and Applications 20(1):100-105 DO!:10.1002/pip.1102 retrieved from www.researchgate.net/publications/228038495_On_the_testing_of_large_PV_arrays on date_may 3,2018.

Mattei M, Notton G, Cristofari G, Muselli M, Poggi P, Calculation of the polycrystalline PV module temperature using a simple method of energy balance. Renew Energy 2006;31:p.553-567 from www.Sciencedirect.com retrieved on 20 July 2018.

Mon.G, Wen. L, Ross. R and Adent. D, Proceedings of the18th IEEE Photovoltaic Specialists Conference, Las Vegas, a)
Mon G. and Ross. R., Proceedings of the 18th IEEE Photovoltaic Specialists Conference, Las Vegas, NV, USA, 1985, pp. 1179–1185. pp. 1142–1149 b).retrieved from https://www2.jpl.nasa.gov/adv_tech/photovol/ppr_81-85/Effect%20of%20T&RH%20on%20Leakage%20-%20PVSC1985.pdf on May 16,2018

Naumann.V,Lausch D, Hähnel A, Bauer J,Breitenstein O, Graff. A, Werner M, Swatek. S, Groβer S, Bagdahn J, Hagendorf C, "Explanation of potential-induced degradation of the shunting type by Na decoration of stacking faults in Si solar cells." Solar Energy Materials &

Solar Cells 120 (2014) 383–389. Retrieved from http://www-old.mpi-halle.mpg.de/mpi/publi/pdf/11827_14.pdf. on date June 17, 2018.

Oh, W, Bae, S, Chan, S. I, Lee, H. S., Kim, D, & Park, N."Potential induced degradation of N-type crystalline silicon solar cells with p+ front junction "retrieved from https://onlinelibrary.wiley.com/doi/epdf/10.1002/ese3.146 on date July 28,2018.

Oh,Wonwook Bae Soohyun, Chan Sung Il, Lee Hae Seok, Kim Donghwan , Park Nochang" Field degradation prediction of Potential induced degradation of crystalline silicon photovoltaic modules based on accelerated test and climatic data." Microelectronics Reliability 76-77(2017) 596-600 retrieved from Sciencedirect.com on June 15, 2018)

Pingel. S, Frank.O, Winkler.M, Daryan.S, Geipel.T, Hoehne. H, Berghold.J, SOLON SE. "Potential Induced degradation of solar cells and panels.' Photovoltaic Specialists conference (PVSC) 2010. 35th IEEE PVSC 2010 June (pp.002817-002822). Retrieved from https://www.researchgate.net/publication/224187548_Potential_Induced_Degradation_of_solar_cells_and_panels on date 12 June 2018.

Qusay Hassan, Jaszczur Marek, Przenzaki Estera, Abdulateef Jasim The PV cell Temperature effect on the energy production and module efficiency" Dec 2016 retrieved from : https://www.researchgate.net/publication/316548825 on 24th July 2018.

Schwingschakl C, Petitta.M, Wagner.JE, Belluardo.G, Moser, D, Castelli,M, Zebisch M and Tetzlaff .A ,"Wind Effect on PV module temperature: Analysis of different techniques for an accurate estimation." European Geosciences Union General Assembly 2013, Energy Procedia 40 (2013)77-86 from www.Sciencedirect.com retrieved on 20 July 2018.

Siddiqui,A.F ,Usama M, Arif. M, Kelley Leah, Dubowsky Steven "Three dimensional thermal modelling of a photovoltaic module under varying conditions" retrieved from https://www.researchgate.net/publication/256854931_Three-dimensional_thermal_modeling_of_a_photovoltaic_module_under_varying_conditions on 26 July 2018.

Singh. H, Sharma, Dr N, Shriwastva A, "Effects of Potential Induced degradation on Solar PV Module based on temperature and humidity." International Journal of Research Volume 05 Issue 04 February 2018 retrieved from https://edupediapublications.org/journals

Skoplaki E, Palyvos JA Operating temperature of photovoltaic modules: A survey of pertinent correlations. Renew Energy 2009; 34: p 23-29 from www.Sciencedirect.com retrieved on 20 July 2018.

Smith R.M, Osterwald. C.R, Gelak E., Kurtz S.R " Outdoor PV Degradation Comparison" Presented at the 35th IEEE Photovoltaic Specialists Conference (PVSC'10) retrieved from https://www.nrel.gov/docs/fy11osti/47704.pdf on August 12,2018.

Swanson R, Cudzinov M, DeCeuster Desai D.,V, Jürgens J., Kaminar N, Mulligan Rodrigues-Barbarosa W.,L, Rose D, Smith D, Terao A, Wilson K. "The surface polarization effect in high efficiency silicon solar cells." 2004 Retrieved from https://us.v-cdn.net/6024911/uploads/attachments/512/6733.pdf on July 16, 2018.

Zhang Y, Sakhuja M,Lim F.J, Tay S, Tan C, Bieri M, Krishnamurthy V, Wang D. Krishnakumar P, Ha J, Zhao Z, Reindl T "The PV System Doctor-Comprehensive diagnosis of PV system installations SNEC 11th International Photovoltaic Generation conference& exhibition,SNEC 2017 scientific Conference 17-20 April 2017, Shangai 2017 energy procedia 130(2017 108-113)

Image 1: Showing a high voltage potential leading anions (negative ions) into migration, away from semiconductor. Source: Yewdall Z, "ask the experts transformerless inverters and PV degradation, Issue #158, December / January 2014 retrieved from https://www.homepower.com/articles/solar-electricity/equipment-products/ask-experts-transformerless-inverters-and-pv. on date July 25, 2018.

Figure 5-6: PID failure, PID free source: https://www.solarassetmanagementeu.com/new-updates-source/new-plant-upgrade-funding-model-could-battle-pid-and-increase-roi.

Figure 7-8 Luo Wei, Khoo Yong Sheng, Hacke Peter, Volker Naumann, Lausch Dominik, Harvey P Steven, Singh Jai Prakash, Chai Jing, Wang Yan, Arm 2016, Potential-induced degradation in photovoltaic modules: a critical review. Energy, Environment and science, Royal society of chemistry. Retrieved from https://www.researchgate.net/.../310666372_Potential-induced_Degradation_in_Photovo... on date June 6, 2018.

6. List of Tables

7. List of Figures

8. Appendix 1

Specifications for PIDBOX are provided below

It is possible in recovery to apply reverse voltage to the module affected by PID using an offset box during the night. Sodium Ions move from the solar cell to the front side of the module after application of voltage in the reverse direction. There are various technologies and applications in solving the PID problem. The best method available is to continuously reduce PID nightly without the costly replacement of the entire module. This is what is expected from the use of Ilumen PIDBoxes as shown below.

Technical data	ILUMEN PID BOX
PV array / inverter input	
Input PV voltage range	80 - 1000 V
Output voltage to ground	**Up to 1250 V**
Maximum PV current / input	
V75	75 A
V100	100 A
V125	125 A
V150	150 A
V200	200 A
V250	250 A
V300	300 A
V350	350 A
Number of independent DC inputs	1
Maximum cable section per busbar	2 x 240 m^2
Maximum output current in operation	16 mA
GRID (AC)	
Nominal AC voltage	110 to 130 V or 220 to 250 V (specify when ordering)
Nominal AC grid frequency	50 to 60 Hz
Power consumption in standby operation	8 W
Typical power consumption in operation	20 W (typically 0,3kWh/day)
Maximum power consumption	25 W
Inrush power	80 W
General data	
Dimensions (W x D x H)	520 x 140 x 550 mm
Weight	16 kg
Operating temperature range	-25 to 60 °C (-13 to 140 °F)
Environmental conditions	IP65 indoor use/outdoor use
Configuration	**one DC-input**
None of the connected solar module poles may become grounded on the PV side, grounding on the inverter side is possible	
Solar cell technology	
This product will function with p-type solar cells. If you want to apply this product to another technology, please contact iLumen	
Various	
Warranty	Up to 20 years
Certificates	www.ilumen.be

Figure 62: Illustrates what a PID box of the type introduced to the site looks like from a consumer perspective.

From laboratory testing a degraded cell from an outdoor test array where the cells were operated positive to ground (Swanson et al. 2004, 4) had an output of 140W, after applying a negative 1000 volts to the cells for one hour, the recovery in output was 203W in the module, the voltage application to the front surface was grounded via a water film.